

ORIGINAL ARTICLE

Cell Fate Determination of the Potato Shoot Apex and Stolon Tips Revealed by Single-Cell Transcriptome Analysis

Chaocheng Guo | Zhuoran Huang | Siyu Luo | Xinyuan Wang | Jiahao Li | Guolong Yu | Yudong Wang | Xu Wang 

Shanghai Collaborative Innovation Center of Agri-Seeds, Joint Center for Single Cell Biology, School of Agriculture and Biology, Shanghai Jiao Tong University, Shanghai, China

Correspondence: Yudong Wang (yudongwang@sjtu.edu.cn) | Xu Wang (xu.wang@sjtu.edu.cn)

Received: 23 June 2024 | **Revised:** 11 February 2025 | **Accepted:** 23 February 2025

Funding: This research was supported by the National Natural Science Foundation of China (32071160, 32161133021), and Shanghai Collaborative Innovation Center of Agri-Seeds Foundation (ZWH2150201/012).

Keywords: phytohormone | potato | single-cell RNA sequencing | stolon | transcription factors

ABSTRACT

Potato (*Solanum tuberosum* L.) is a starch-rich crop with two types of meristematic stems: the shoot and stolon. Shoots grow vertically, while stolons grow horizontally underground and produce tubers at their tips. However, transcriptional differences between shoot and stolon cells remain unclear. To address this, we performed single-cell RNA sequencing of the shoot apex and stolon tip, generating a comprehensive transcriptional landscape. We identified 23 distinct cell clusters with high cell heterogeneity, including cell-specific genes and conserved genes with cell-specific expression patterns. Hormone-related genes, particularly those involved in auxin and gibberellin pathways, exhibited distinct patterns among shoot and stolon cells. Meristematic cells were re-clustered based on the expression of *StPOTH15*, a homolog of *SHOOT MERISTEMLESS* (*STM*) in Arabidopsis. Co-expression networks of transcription factors identified the key transcription factors involved in stolon development. We also constructed developmental trajectories for xylem and phloem development using key vascular genes, including *MP*, *XCP1*, *PP2A1* and *SEOR1*. Comparative analysis with Arabidopsis highlighted significant differences in cell type-specific transcript profiles. These results provide insights into the transcriptional divergence between potato shoot and stolon, and identify key transcription factors co-expressed with *StPOTH15* that can be used to explore their roles in stolon development.

1 | Introduction

Potato (*Solanum tuberosum* L.) is one of the most essential starch-rich crops worldwide, providing a valuable source of starch, storage proteins, vitamins and dietary antioxidants. The development of stems in potatoes can be divided into two types according to their position and function. The shoot (or main stem) grows aboveground, producing leaves and flowers with high cell differentiation activity in the shoot apex. The diageotropic shoot is a

stem with strongly elongated internodes known as the stolon growing horizontally underground and produces tubers at the tips (Struik 2007). The number and size of the tubers are tightly associated with the degree of stolon branching, which is in turn influenced by multiple environmental and genetic factors (Celis-Gamboa et al. 2003; Pasare et al. 2013).

Stolon development, occurring before tuber initiation, is a complex process that can be influenced by multiple factors, including

© The Author(s) 2024. Published by Oxford University Press. This is an Open Access article distributed under the terms of the Creative Commons Attribution License <https://creativecommons.org/licenses/by/4.0/>, which permits unrestricted reuse, distribution, and reproduction in any medium, provided the original work is properly cited.

environmental factors and endogenous hormones (Kumar and Wareing 1972). Environmental factors, such as light and temperature, induce *SELF PRUNING 6A* (*StSP6A*) expression to promote potato stolon development and tuberization (Hastilestari et al. 2018; Lehretz et al. 2019; Navarro et al. 2011; Nicolas et al. 2022; Park et al. 2022). A study with *DR5::GUS* transgenic potato showed a strong auxin (or indole-3 acetic acid) signal in the vascular tissues of the swelling stolon tip, demonstrating that this endogenous hormone can stimulate potato stolon formation and tuberization (Roumeliotis, Kloosterman, et al. 2012). Upregulation of the auxin-responsive gene *StARF6* can promote the transformation of the stolon tips cells from longitudinal to transverse division, which is a key signal for further tuberization (Faivre-Rampant et al. 2004). Similarly, overexpression of the auxin biosynthesis gene *TMS1* increased the endogenous auxin content to further promote tuber yield (Kolachevskaia et al. 2015). In addition, a higher gibberellin level in the stolon promotes stolon elongation, whereas a lower gibberellin level is favourable for the stolon-to-tuber transition process (Roumeliotis, Kloosterman, et al. 2012; Xu et al. 1998). Upregulated expression of the gibberellin 2-oxidase gene (*StGA2ox1*) was observed at the stolon tips during the early stages of stolon development in the transition from a non-swelling to swelling stolon, suggesting that a reduction of gibberellin to facilitate this process (Kloosterman et al. 2007). Similarly, *StGA3ox2* showed high expression in the non-swelling stolon tips, and its RNA interference in transgenic potato resulted in the production of more tubers (Bou-Torrent et al. 2011; Roumeliotis et al. 2013). Moreover, strigolactone has been found to play a role in stolon development (Pasare et al. 2013; Roumeliotis, Kloosterman, et al. 2012). However, the specific impacts of these hormones on different cell types and the influence of other hormones on stolon development remain to be elucidated.

Single-cell RNA sequencing (scRNA-seq) is a powerful technique to investigate the heterogeneity of different tissues at the single-cell level in various plant species, including Arabidopsis, rice, maize, poplar, soybean and cotton (Chen et al. 2021; Q. Liu et al. 2021; Z. Liu et al. 2023; Satterlee et al. 2023, 2020; X. Sun et al. 2022; Y. Sun et al. 2023; Y. Wang et al. 2021; T. Q. Zhang, Chen, Liu, et al. 2021; T. Q. Zhang, Chen, and Wang 2021; T. Q. Zhang et al. 2019). One of the primary applications of scRNA-seq in plants is to identify and characterize cell types in diverse plant tissues. The most well-studied plant tissue cells from a transcription perspective are root cell types, which have been extensively profiled in various model and crop species, including Arabidopsis, rice, maize and wheat (Marand et al. 2021; Y. Wang et al. 2021; Wendrich et al. 2020; L. Zhang et al. 2023; T. Q. Zhang et al. 2019). These analyses illustrated the developmental diversity and differentiation trajectories of different cell types in the root, including epidermal, exodermal, cortex and root hair cells (L. Zhang et al. 2023; T. Q. Zhang, Chen, Liu, et al. 2021). Transcriptomes of various cell types in the shoot and leaf tissues have also been examined (X. Sun et al. 2022; T. Q. Zhang, Chen, and Wang 2021). Comparison of the transcriptomes between root and shoot cell types revealed opposing expression patterns and differentiation in the epidermal and vascular tissues in Arabidopsis (T. Q. Zhang, Chen, and Wang 2021). Moreover, scRNA-seq has been used to compare the transcriptional differences between wild-type and mutant plants harbouring mutations at a single locus, resulting in the loss of specific cell types (Shahan et al. 2022; D. Wang

et al. 2023). For instance, scRNA-seq analysis of the cotton ovules showed that the fuzzless/lintless mutant (*fl*) lost the fibre-specific cell type C3 compared with the wild type, resulting in the fibre loss phenotype (D. Wang et al. 2023). ScRNA-seq also enables the determination of cellular heterogeneity in plant responses to various stimuli, including phytohormones (cytokinin, brassinosteroid and jasmonic acid) and heat stress (Nguyen et al. 2023; Nolan et al. 2023; X. Sun et al. 2022; B. Yang et al. 2021). Thus, scRNA-seq has the potential for exploring intricate facets of transcription regulation in plants.

Here, we performed scRNA-seq on the shoot apex and stolon tips of potato to obtain a comprehensive transcriptional landscape of shoot and stolon cells. We identified potential cell-type-specific marker genes and classified these heterogeneous cell populations into five major cell types, including epidermal cells, mesophyll cells, proliferating cells, vascular cells and meristematic cells. We also compared the divergence in expression pattern between the shoot and stolon cells in a cell type-specific manner. We further reconstructed the differentiation trajectories of phloem and xylem cells based on their transcriptome profiles. Finally, we conducted a cross-species analysis based on the shoot cell atlases of potato and *Arabidopsis* to gain insight into the conservation and divergence of shoot cells during the evolution of potato. Overall, our study provides comprehensive single-cell transcriptome data of shoot and stolon cells, which can facilitate exploration of the mechanism of tuberization in potato for potential agricultural applications.

2 | Materials and Methods

2.1 | Plant Growth Condition and Protoplast Isolation

The potato cultivar ‘*Atlantic*’ was grown in plastic pots (10 cm × 10 cm) with nutrient soil in a climate-controlled greenhouse. The photoperiod was established under a long-day condition of 16 h light/8 h dark with 22°C light/20°C dark. When the stolon formed at a non-swelling stage (Roumeliotis, Kloosterman, et al. 2012), the stolon tips (0.5 cm) and the according shoot apex (0.5 cm) for further protoplast isolation (Supporting Information S1: Figure S1). For protoplast isolation, the stolon tips and shoot apices were cut into small pieces of approximately 1 mm and then incubated in enzyme solution (1.5% cellulase R10, 1% macerozyme R10, 0.4 M mannitol, 0.1 M 4-morpholineethanesulfonic acid, 10 mM KCl, 10 mM CaCl₂ and 0.1% bovine serum albumin, pH 5.7) for 4 h at 28°C in a shaking incubator with 70 rpm for protoplast isolation. The protoplasts were filtered with a 40 µm strainer and then washed twice with 0.6 M mannitol solution. The protoplast viability was determined by 0.2% trypan blue staining. The samples with protoplast viability ≥ 80% were used for further scRNA-seq library construction and sequencing.

2.2 | Preparation for scRNA-seq Sequencing

The single-cell suspensions were loaded on a Chromium Single Cell Instrument (10× Genomics, Pleasanton, CA, USA) to

generate single-cell Gel Beads-in-emulsions. The scRNA-seq libraries were prepared using randomly interrupted whole-transcriptome amplification products to enrich the 3' end of the transcripts linked with the cell barcode and unique molecular identifier (UMI). All remaining procedures, including library construction, were performed according to the manufacturer's standard protocol (Chromium Single Cell 3' v3.1). The libraries were sequenced on an Illumina NovaSeq. 6000 sequencing platform with 150 bp paired-end reads. The sequencing was performed by Majorbio Co. Ltd. (Shanghai, China). The raw sequence data used in this study are available at the National Genomics Data Center (NGDC; <https://ngdc.cncb.ac.cn/>) under Bioproject accession number PRJCA020216.

2.3 | Pre-Processing of Raw scRNA-seq Data and Doublet-Detection

The raw scRNA-seq reads were aligned to the potato genome (DM Version 6.1) by Cell Ranger 3.0.1 (10x Genomics). The genome and gene annotation file of the potato were downloaded from the SpudDB database (<http://spuddb.uga.edu/index.shtml>). We first used the function 'cellranger mkref' to generate the reference index and the function 'cellranger count' to generate the expression matrix for further cluster analysis. Doublets in each scRNA-seq data set were identified and removed by DoubletFinder (v.2.0.2) software (McGinnis et al. 2019). In brief, to identify the optimal neighbourhood size (pK value), the function 'paramSweep_v3' was used to scan the K parameter and the function 'find.pK' was subsequently used to obtain the maximum pK value, defined as the optimal pK value. The number of artificial doublets (pN) was set to 0.25 and the number of expected real doublets (nEXP) was assumed to be 5% of the number of all cells in the scRNA-seq data set. Finally, the function 'doubletFinder_v3' was used to label all cells and only those labelled as 'Singlets' were retained for further analysis. To evaluate the reproducibility of the data, each experiment was conducted with two biological replicates.

2.4 | Cell Clustering and Identification of Cell Type Marker Genes

Downstream analysis of the scRNA-seq data was performed with the Seurat V3.1.1 package in R language (Satija et al. 2015). For quality control, the cells with UMI counts ranging from 500 to 50 000 and feature counts ranging from 500 to 10 000 were retained for further data processing. The features expressed in less than three cells were removed. The gene expression matrix was processed as described in the Arabidopsis shoot apex. The gene expression data were normalized by the 'NormalizeData' function with the LogNormalize method and a scale factor of 1000. The 'FindVariableFeatures' function was used to identify the top 3000 features with the vst method. The batch effects between samples were corrected by the Harmony package (Korsunsky et al. 2019). Cell clustering was conducted by the Louvain method with a resolution of 0.9. The tSNE and Uniform Manifold Approximation and Projection (UMAP) methods were both used to visualize the distribution of cells. Based on the cell clusters, the 'FindAllMarkers' function was used to

identify the cluster-enriched marker genes with a Wilcoxon test. The genes that showed a 1.5-fold [\log_2 fold change (FC) > 0.58] greater expression level than the corresponding genes in the other clusters and had a minimum fraction value of at least 0.25 were defined as cluster-enriched marker genes. The clusters were assigned to different cell types according to known representative marker genes of the homologous genes of *Arabidopsis*. The three-dimensional (3D) UMAP plot was constructed using the R package 'plotly'. The effects of protoplasting genes were evaluated using the 'PercentageFeatureSet' function based on the public protoplasting genes in *Arabidopsis* (Yadav et al. 2009).

2.5 | Comparison of Shoot and Stolon Cell Types

The correlation coefficients of different cell types between shoot and stolon cells were calculated by the function 'rcorr' of the R package 'Hmisc'. The expression heatmap was visualized using the R package 'pheatmap'. The dot plots of cell-specific gene expression were constructed using the R package 'ggbeeswarm'. The significance of differential expression for each gene between shoot and stolon cells was calculated with the 't.test' function. The shoot-specific and stolon-specific genes were defined as genes with $|\log_2 \text{FC}| > 0.58$ and $p < 0.05$. The conserved genes were identified with the function 'FindConservedMarkers'.

2.6 | Sub-Clustering of Meristem, Xylem and Phloem Cells

To comprehensively compare the difference in meristem cells (MCs) between the shoot and stolon, we selected the cells that had a *StPOTH15* expression level > 0 for further sub-clustering, which was performed according to the methods described in a previous study on the shoot apex of *Arabidopsis* (T. Q. Zhang, Chen, and Wang 2021). We defined these cells with expression of *StPOTH15* as *StPOTH15*⁺ differentiating cells. The raw counts of these *StPOTH15*⁺ cells were imported into Seurat to create a new Seurat object. The processes of data normalization and cell clustering on these *StPOTH15*⁺ cells were performed as described above. Likewise, the sub-clustering of xylem and phloem cells only focused on the cells of clusters 14 and 16, respectively. In addition, the parameters of the total number of PCs (npcs), dimensions (dims) and resolution were specifically adjusted according to the different cell types (meristem cells: dims = 20, nmps = 20, resolution = 0.5; xylem cells: dims = 30, nmps = 30, resolution = 0.4; phloem cells: dims = 30, nmps = 30, resolution = 0.4). The cluster-enriched genes were calculated using the 'FindAllMarkers' function with the following parameters: Wilcoxon rank sum test; above 0.58-fold difference ($\log_{10} \text{FC} \geq 0.58$), at least 0.1-fold minimum fraction ($\text{min.pct} \geq 0.1$).

2.7 | Identification of Cell-Type-Specific Regulons and Co-Expression Network of *StPOTH15*

The 1969 TFs of potato were predicted through the Transcription Factor Prediction tool on the plantTFDB website (<http://planttfdb.org>)

plantfdb.gao-lab.org/prediction.php). The motifs data of potato were collected from the CIS-BP data set (<http://cisbp.ccb.utoronto.ca/>) and JASPAR website (<https://jaspar.genereg.net/>). The co-expression network of *StPOTH15* was constructed through the Pearson Correlation coefficient (PCC) value. The top 20 co-expressed genes of *StPOTH15* were visualized with the ‘gggraph’ package in R.

2.8 | Pseudotime and Gene Modules Analyses

The developmental trajectories of xylem and phloem cells were determined using Monocle3 (version 1.0.0). First, the raw gene matrix of xylem and phloem cells was extracted from the Seurat object by the function ‘GetAssayData’ and further transformed into a Monocle3 object by the function ‘new_cell_data_set’. The trajectory analysis was performed as previously described. In brief, we used the functions ‘preprocess_cds’ and ‘align_cds’ to normalize and process the raw data, and then used the function ‘reduce_dimension’ with the UMAP method to transform the data to a lower dimension. Subsequently, the cells were clustered into different groups by the function ‘cluster_cells’, while the trajectory was inferred with the function ‘learn_graph’. The dynamic differentially expressed genes among the developmental trajectories were obtained by the function ‘graph_test’ with the significance set as a *q*-value < 0.05. The gene modules of the expressed genes with similar functions were identified by the function ‘find_gene_modules’. The combination of expression in different modules was conducted by the function ‘aggregate_gene_expression’ and further visualized by the R package ‘pheatmap’. The distribution of pseudotime value was visualized by the R package ‘ggbeeswarm’.

2.9 | Pairwise Comparison Between Potato and Arabidopsis or Rice

The published scRNA-seq data set of the shoot apex in Arabidopsis (BioProject PRJCA003094) was downloaded from the Beijing Institute of Genomics Data Center (<http://bigd.big.ac.cn>) (T. Q. Zhang, Chen, and Wang 2021). Three published datasets of the Arabidopsis root were downloaded from the National Center for Biotechnology Information (NCBI; GSE123818, GSE141730 and GSE123013), and integrated into a comprehensive landscape of the root tissue at the single cell level (Denyer et al. 2019; Ryu et al. 2019; Wendrich et al. 2020). The published scRNA-seq data set of root tip in rice was downloaded from NCBI under the project ID PRJNA706435 (T. Q. Zhang, Chen, and Wang 2021). The transcriptional similarity of cell types between different tissues and species was evaluated by MetaNeighbor software using the gene expression data of the single-copy genes, as previously described (Crow et al. 2018; Li et al. 2023). A higher MetaNeighbor score indicates higher transcriptional similarity between cell types or tissues. The single copy genes between potato and Arabidopsis or rice were identified by OrthoFinder version 2.4.0 (Emms and Kelly 2019). The Sankey plots of shared marker genes across homologous cell types between potato and Arabidopsis or rice were plotted by the R package ‘networkD3’.

2.10 | Integrative Analysis of scRNA-seq Datasets of the Potato and Arabidopsis Shoot Apex

To better compare the cell heterogeneity across homologous cell types in the shoot apex between potato and Arabidopsis, only the shoot cells of potato were integrated with those of Arabidopsis into a UMAP plot. The function ‘SelectIntegrationFeatures’ was used to select the top 2000 features, and the function ‘FindIntegrationAnchors’ was used to obtain integration anchors across all samples. Furthermore, the function ‘IntegrateData’ was used to combine the datasets based on the selected anchor set with default additional arguments. The integrated data were further processed with standard normalization and cell clustering using 20 principal components. The functions ‘ScaleData’ and ‘RunPCA’ were then performed on the integrated assay to compute the 20 principal components. UMAP dimensionality reduction was carried out and a shared nearest-neighbour (SNN) graph was constructed using the dimensions 1:20 as input features and default principal component analysis reduction. Clustering analysis was performed on the integrated assay at a resolution of 0.5.

The transcriptional similarity across homologous cell types in the shoot apex between potato and Arabidopsis was determined according to the Pearson correlation method based on the average expression levels of each cell type aggregated with the function ‘AverageExpression’. The correlation coefficient heatmap was generated with the ‘pheatmap’ package in R. The differentially expressed genes and conserved genes across homologous cell types in the shoot apex between potato and Arabidopsis were identified by the ‘Seurat’ package in R with the functions ‘FindMarkers’ and ‘FindConservedMarkers’, respectively. The fold difference was the threshold to identify genes with high divergence (> 5-fold), moderate differences (2- to 10-fold), and small differences (< 2-fold) in expression levels.

2.11 | Gene Functional Enrichment and Pathway Analysis

The Gene Ontology (GO) enrichment analysis of cluster-enriched genes was conducted by the ‘ClusterProfiler’ package in R (Wu et al. 2021). The *p* value was adjusted with the Benjamini Hochberg (BH) method. The dot plots or bar plots of GO results were constructed in R with the ‘ggplot2’ package.

2.12 | RNA Isolation and Reverse Transcription-Quantitative Polymerase Chain Reaction (RT-qPCR)

RNA was isolated from ~0.5 cm of stolon tips in the no-swelling stage and from the shoot apex collected ~0.5 cm from the shoot apical region using RNAiso Plus (Takara, Japan) following the manufacturer’s instructions. The RNA was reverse-transcribed to complementary DNA (cDNA) with a QuantiTect Reverse Transcription Kit (Qiagen, Germany). All RT-qPCRs were conducted with a SYBR premix Ex Taq kit (Takara, Japan) on the CFX384 Touch Real-Time PCR Amplification System (Bio-Rad, USA). The relative expression levels were normalized

against the reference potato actin gene *StActin* (*Soltu.DM.11G008990*) as previously described (Abelenda et al. 2019). Primers used for RT-qPCR are listed in Supporting Information S2: Table S1.

2.13 | RNA In Situ Hybridization

Fresh shoot apex and stolon tip were harvested following the same procedures used for scRNA-seq sample collection and were fixed in FAA solution for 24 h at 4°C. The tissue blocks were then cut into approximately 3 mm thick, dehydrated using a graded alcohol, cleared with xylene, and embedded in paraffin. The paraffin-embedded samples were sectioned into 6 µm slices. These sections were treated with xylene, dehydrated again with graded alcohol, and digested with 200 µg/mL of protease K. The sections were incubated with these probes overnight at 40°C. After washing, they were incubated with an alkaline phosphatase-conjugated anti-digoxin antibody at 40°C for 50 min and detected using a nitro-blue tetrazolium/5-bromo-4-chloro-3'-indolylphosphate solution. The probe informations are listed in Supporting Information S2: Table S1.

2.14 | Dual-Luciferase (dual-LUC) Assay

The luciferase assay for transcription factors and the promoter of StPOTH15 was conducted in tobacco leaves. For the vector, the coding sequences of transcription factors were fused into pCAMBIA1301 vector to serve as the effector. The 2 kb promoter sequences of StPOTH15 were cloned into pGreen II 0800 to act as reporter. The pCAMBIA1301 empty vector was used as a negative control. The Firefly LUC and REN activities were measured using the dual-luciferase reporter assay kit (Promega). At least three independent experiments were performed for each transcription factor.

3 | Results

3.1 | Generation of a Single-Cell Transcriptional Landscape of Potato Stolon Tip and Shoot Apex

To generate comprehensive transcriptome data of shoot apices and stolon tips in potato, we isolated the protoplasts from the new-born stolon tips (~0.5 cm in length from the stolon tips) and shoot apex (~0.5 cm from the apical region) of the tetraploid potato cultivar ‘Atlantic’, and then performed transcriptomic sequencing at the single-cell resolution on the 10x Genomic scRNA-seq platform. To evaluate the reproducibility of the data, each experiment was conducted with two biological replicates. Through integration of the transcriptome data from of stolon and shoot cells, we obtained a cell atlas with 35 048 high-quality cells for further analysis, containing 13 177 high-quality stolon cells (6771 cells in Stolon_R1 and 6406 cells in Stolon_R2) in the stolon tips and 21 871 high-quality shoot cells (10 993 cells in Shoot_R1 and 10 878 cells in Shoot_R2) in the shoot apex (Supporting Information S2: Table S2). The protoplasting genes had little effects on the clustering (Supporting Information S1: Figure S2). The data produced by scRNA-seq

were highly correlated with the bulk RNA-seq data, indicating the overall reliability of the scRNA-seq data (Supporting Information S1: Figure S3).

Using the uniform manifold approximation and projection (UMAP) method, we classified these 35 048 cells into 23 distinct clusters (Figure 1a; Supporting Information S1: Figure S4). Clusters 2, 3, 5, 6, 7, 8, 9, 10, 18, 20 and 21 harboured a higher proportion (>70%) of shoot cells than stolon cells, whereas clusters 0, 4, 12, 15, 16 and 22 exhibited the opposite trend, implying cell heterogeneity among different tissues in potato (Figure 1b). To compare the difference among clusters, we identified a series of 2541 marker genes with high expression in one or two clusters compared with all other clusters. Cluster 10 had the highest number (572) of marker genes (Supporting Information S1: Figure S5a). A total set of 1311 genes showed strong cluster-specific expression patterns in a single cluster, whereas 1230 marker genes exhibited high expression in more than one cluster (Supporting Information S1: Figure S5b and Supporting Information S2: Table S3).

3.2 | Identification of Distinct Cell Types in the Stolon Tip and Shoot Apex

Because of the limitation of known marker genes in the stolon, we first compared and investigated the homologs of known marker genes in *Arabidopsis thaliana*, whose functions and expression patterns have been well studied (Supporting Information S2: Table S4). Using these homologous genes in potato, we distinguished the cells in the 23 clusters into five major cell types similar to the classification in *Arabidopsis*, except for guard cells (GCs) (Figure 1c; Supporting Information S1: Figure S6). We speculated that the tissues of GCs were not yet mature in the shoot apex owing to low expression of GC marker genes in several cells, including *ALMT12-2* (*Soltu.DM.08G001280*), *EPF1* (*Soltu.DM.12G028300*), *FAMA* (*Soltu.DM.05G023840* and *Soltu.DM.09G028830*), *MYB60* (*Soltu.DM.10G025860*), and *SCAPI* (*Soltu.DM.11G002690*) (Supporting Information S1: Figure S7a). Moreover, these GC marker genes exhibited expression in the epidermal cell (EC)-related clusters, including clusters 12, 13, 15 and 19 (Supporting Information S1: Figure S7b). Mesophyll cells (MEs) characterized seven clusters (cluster 1, 3, 5, 6, 7, 9 and 10) with high expression of *BLUE-COPPER-BINDING PROTEIN* (*BCB*, *Soltu.DM.07G003570*), *CHLOROPHYLL A/B BINDING PROTEIN 1* (*CAB1-1* and *CAB1-3*, *Soltu.DM.02G013810* and *Soltu.DM.02G014000*), *RUBISCO SMALL SUBUNIT 3B* (*RBCS3B-1*, *Soltu.DM.02G025810*), *GERMIN 3* (*GER3-2*, *Soltu.DM.07G012540*), and *PHOTOSYNTHETIC NDH SUBCOMPLEX L1* (*PNSL1*, *Soltu.DM.10G016620*). The expression of key epidermal development-related genes, such as *PROTODERMAL FACTOR 1* (*PDF1-1* and *PDF1-3*, *Soltu.DM.07G021960* and *Soltu.DM.12G028710*), *DEFECTIVE IN CUTICULAR RIDGES* (*DCR*, *Soltu.DM.03G018100*), *FIDDLEHEAD* (*FDH*, *Soltu.DM.08G015830*), and *EMBRYO SAC DEVELOPMENT ARREST 17* (*EDA17-1*, *Soltu.DM.03G036380*), showed high specificity in clusters 0, 2, 8, 12, 13, 15, 18 and 19, which were considered to be characterized by ECs. Cluster 17 was assumed to reflect the proliferating celArabidopsis (PCs) owing to the high expression of PC marker genes, such as *FIZZY RELATED 3* (*FZR3*, *Soltu.DM.06G008810*), *SYNTAXIN OF PLANTS 111* (*SYP111*, *Soltu.DM.06G014770*), *3x HIGH MOBILITY GROUP-BOX 2* (*3xHMG-box 2-1*, *Soltu.DM.08G028810*), and

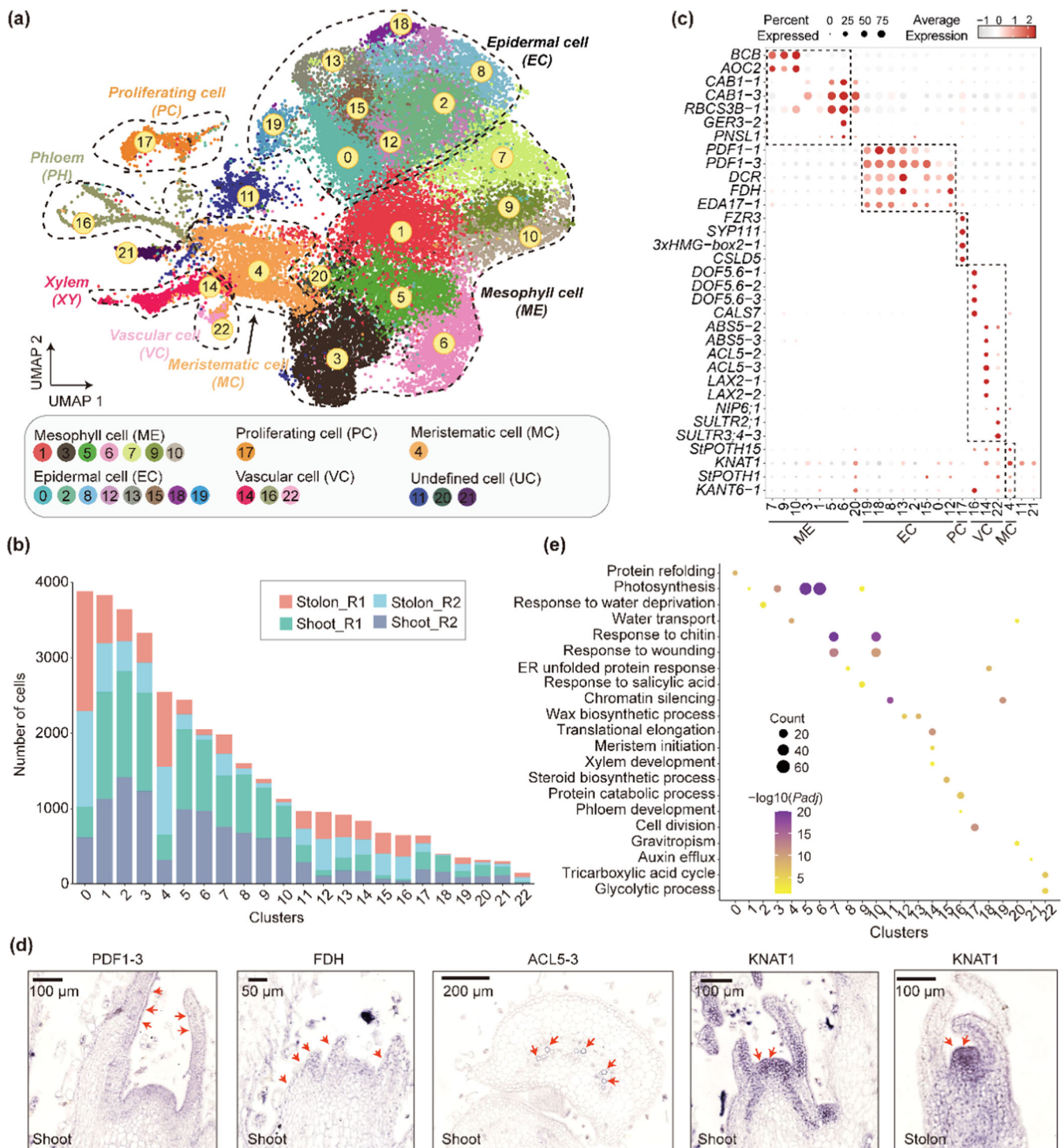


FIGURE 1 | Cell heterogeneity in the shoot apex and stolon tip of potato. (a) UMAP visualization of 23 distinct cell clusters from 35 048 cells in the shoot apex and stolon tip. (b) Numbers of cells from two replicates each of shoot and stolon samples among the 23 cell clusters. (c) Expression pattern of representative cell-specific marker genes in 23 cell clusters. The size of dots indicates the proportion of cluster cells expressing a given gene. (d) RNA in situ hybridization of marker genes in epidermal cells, vascular cells, and meristematic cells. (e) Gene Ontology enrichment analysis of the cluster-specific genes.

CELLULOSE SYNTHASE-LIKE D5 (CSLD5, *Soltu.DM.09G023860*). The vascular cells (VCs) were represented by three clusters (14, 16 and 22), covering significantly enriched xylem-specific and phloem-specific genes. The companion cells (CCs) were mixed with sieve elements in the phloem as multiple CC and sieve element-related marker genes were highly expressed in cluster 16 (Supporting

Information S1: Figure S8a and S8b). Furthermore, the xylem-related genes, such as *ABNORMAL SHOOT 5* (*ABS5-2* and *ABS5-3*, *Soltu.DM.04G001370* and *Soltu.DM.04G008700*), *ACUALIS 5* (*ACL5-2* and *ACL5-3*, *Soltu.DM.08G012380* and *Soltu.DM.09G024210*), and *LIKE AUXIN RESISTANT 2* (*LAX2-1* and *LAX2-2*, *Soltu.DM.01G050890* and *Soltu.DM.10G017220*) were

overrepresented in cluster 14. Similarly, cluster 22, designated $VC^{P/X}$ to reflect VSs excluding the phloem and xylem, contained bundle sheath-associated genes, including *NOD26-LIKE INTRINSIC PROTEIN 6;1* (*NIP6;1*, *Soltu.DM.03G031200*), *SULFATE TRANSPORTER 2;1* (*SULTR2;1*, *Soltu.DM.04G021850*), and *SULTR3;4-3* (*Soltu.DM.12G010700*). Cluster 4 was considered to reflect MCs with high expression of *POTATO HOMEOBOX 15* (*StPOTH15*, *Soltu.DM.02G020620*), *KNOTTED-LIKE FROM ARABIDOPSIS THALIANA 1* (*KNAT1*, *Soltu.DM.04G031920*), *StPOTH1* (*Soltu.DM.05G009240*), and *KNAT6-1* (*Soltu.DM.01G040260*), despite the expression of meristematic associated genes in other cell types. A previous study showed that *StPOTH15*, a homolog of *SHOOT MERISTEMLESS (STM)* in Arabidopsis (Endrizzi et al. 1996), was widely expressed in the MCs of both the shoot apex and stolon tips. Apart from the MCs, the vascular tissues also exhibited high expression of *StPOTH15*, supporting that cluster 4 includes MCs. For validation, we selected several genes for *in situ* experiments (Figure 1d). The results confirmed that the expression patterns of these genes were consistent with our expectations. For instance, marker genes for epidermal cells, such as *PDF1-3* and *FDH*, exhibited strong signals in the epidermal cells. The gene *KNAT1* displayed robust signals in both shoot and stolon meristematic regions. Additionally, the vascular gene *ACL5-3* was found to be specifically expressed in xylem cells.

To investigate the potential functions of these cell clusters, we performed GO enrichment analysis for the marker genes of each cluster. As a result, we distinguished the possible functions of these annotated cell types, which were highly similar to the corresponding cell types (Figure 1e). For instance, clusters 3, 5, 6 and 9, which were annotated as MEs, were enriched in the term named ‘photosynthesis’, suggesting that these cells may play a crucial role in photosynthesis in potato. Moreover, the GO term ‘wax biosynthesis process’ was enriched in EC-related clusters, including clusters 12 and 13. Of note, we identified meristem-related GO terms, such as ‘translational elongation’ and ‘meristem initiation’, enriched in the xylem cluster, suggesting a potential link to cell differentiation in the xylem of potato. The vascular tissues were highly enriched in the GO terms ‘tricarboxylic acid cycle’ and ‘glycolytic process’, implying a role of energy metabolism. Interestingly, the unannotated cluster 20 was related to ‘gravitropism’, suggesting a function of the shoot endodermis cells in shoot gravitropic response, as has been reported for Arabidopsis (T. Q. Zhang, Chen, and Wang 2021). We also identified key genes with high expression levels in cluster 20, which were homologous to genes reported to be related to shoot gravitropism in Arabidopsis, with high expression in cluster 20, such as *LAZY1* (*Soltu.DM.05G012170*), *TAC1* (*Soltu.DM.01G035400*), and *AT3G48550* (*Soltu.DM.03G026800*) (Supporting Information S1: Figure S9a and S9b).

3.3 | Photosynthesis and Phytohormones Determine the Transcriptional Divergence Between the Shoot Apex and Stolon Tip at the Single-Cell Resolution

To investigate the transcriptional diversity between the two meristematic tissues (shoot apex and stolon tip), we compared the same cell types in the two tissues to determine conserved and divergent genes during the development according to the

distribution of cells by origin and cell type (Figure 2a,b). The proportion of shoot cells in MEs and PCs was higher than that in stolon cells, while the proportions of shoot cells among MCs, phloem and $VC^{P/X}$ were lower than those in stolon cells. To investigate the transcriptional similarity between shoot and stolon cells, we calculated the Pearson correlation coefficient (PCC) among all cell types based on the average expression level of each cell type. Different cell types within the same tissue exhibited high PCC values (average $PCC_{shoot} = 0.82$, average $PCC_{stolon} = 0.80$; Figure 2c). When comparing the same cell type between shoot and stolon cells, all comparisons had a PCC value above 0.7, especially the xylem ($PCC_{XY} = 0.87$) and phloem ($PCC_{PH} = 0.82$). These results implied high transcriptional similarity among these cell clusters between shoot and stolon cells.

To further examine these differences among different cell types, we identified shoot-specific genes, stolon-specific genes and genes with conserved expression for specific cell types. We found significant differences between shoot-specific and stolon-specific genes in ECs and MEs, whereas there was more conserved expression between the tissues in PCs and the xylem (Figure 2d; Supporting Information S2: Table S5). The conserved genes of each cell type were mostly identified as marker genes involved in the development process for each tissue (Figure 2e; Supporting Information S2: Table S6). For example, *PDF1* was reported to function as a key regulator of ECs in the Arabidopsis shoot apex (Abe et al. 2001), and its potato ortholog, *PDF1-3* (*Soltu.DM.12G028710*), was specifically expressed in the ECs of both the shoot and stolon (Figure 2f). *APL* (*Soltu.DM.12G020640*), which was reported to play a role in phloem development (Bonke et al. 2003), also exhibited high expression in the phloem of both the potato shoot and stolon.

Furthermore, we compared the divergent genes based on their transcriptional difference and determined these tissue-specific genes related to phytohormones and photosynthesis based on GO enrichment analysis (Supporting Information S1: Figure S10a). Several GO terms, including ‘photosynthesis’ and ‘proteasomal ubiquitin-independent protein catabolic process’, were enriched in almost all cell types in the shoot- and stolon-specific genes, respectively, indicating that photosynthesis plays a crucial role in the differentiation of these cells. We then performed GO analysis to investigate the potential function of the conserved genes for each cell type. The top GO terms were related to fundamental biological processes corresponding to the respective roles of each cell type in plant development (Supporting Information S1: Figure S10b). For instance, the ECs were enriched in ‘cuticle development’, ‘lipid catabolic process’, ‘lipid transport’ and ‘wax biosynthetic process’, whereas the PCs were mainly involved in terms related to the cell cycle, such as ‘cell cycle’, ‘cell division’ and ‘mitotic cell cycle’. The VC-related cell types, including the xylem, phloem and $VC^{P/X}$, were mainly associated with terms related to transport and photosynthesis, including ‘photosynthesis’, ‘water transport’, ‘phenylpropanoid metabolic process’ and ‘response to wounding’.

A total of 19 genes related to photosynthesis showed significant expression differences between the shoot and stolon cells (Figure 2g). For instance, the photosynthesis gene *StCAB1-15* (*Soltu.DM.03G004830*) was highly expressed in all shoot cells, especially MEs. *StFAD5* (*Soltu.DM.03G030790*), which encodes

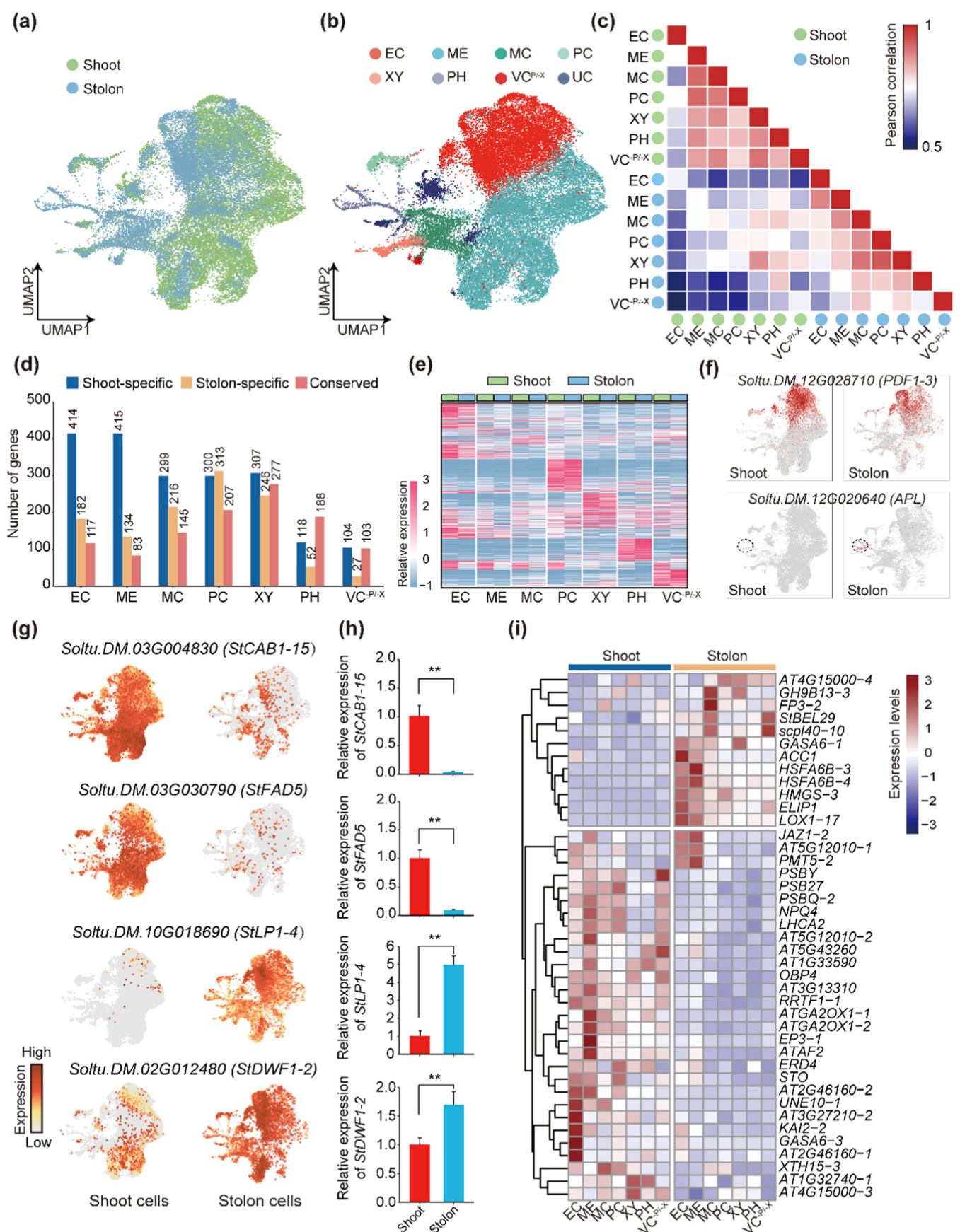


FIGURE 2 | Legend on next page.

an integral chloroplast membrane protein, showed more dominant expression in the MEs among the shoot cells compared to the stolon cells, indicating its potential role in chlorophyll synthesis. In contrast, the ethylene-associated gene *StLP1-4* (*Soltu.DM.10G018690*), which is mainly located in the cell wall of ECs (Thoma et al. 1993; H. Wang et al. 2016), showed higher expression in the stolon than in the shoot. The brassinosteroid (BR)-associated gene *DWARF 1* (*StDWF1-2*, *Soltu.DM.02G012480*) was also more highly expressed in stolon cells than in shoot cells (Du and Poovaiah 2005). These tissue-specific expression patterns were further validated according to their relative expression levels with bulk tissues (Figure 2h). Moreover, we found that the light response network showed diverse expression patterns. A total of 41 target genes of *ELONGATED HYPOCOTYL5* (*HY5*) and phytochrome-interacting factors (PIFs) showed cell type-specific expression patterns, especially in ECs and MEs (Figure 2i). *HY5/HYH* are transcription factors (TFs) with a positive regulatory role on photomorphogenesis, whereas PIFs are negative effectors of this process (Gangappa and Botto 2016; Han et al. 2023; Leivar and Quail 2011). Among them, 12 genes showed expression dominance in the cell types of the stolon, such as *StBEL29*, *ACC1* and *LOX1-17*. A previous study indicated that *StBEL29* might cooperate with a KNOX partner to repress *StSP6A* and inhibit tuber formation, suggesting its important role in stolon development (Ghate et al. 2017). *ACC1* encodes a key enzyme in the biosynthesis of cuticular waxes (Lü et al. 2011), which was consistent with its high expression in ECs of the stolon. Collectively, these results implied that light signalling networks are commonly divergent between the shoot and stolon along with cell type-specific expression patterns.

3.4 | Divergent Hormones Biosynthesis and Responses Between Shoot and Stolon Cells

Previous studies showed that phytohormones are involved in the regulation of various aspects of development and growth in potato, especially tuber initiation and sprouting (Hartmann et al. 2011; Kloosterman et al. 2007; Roumeliotis, Kloosterman, et al. 2012). Therefore, we investigated the expression of genes associated with the biosynthesis and responses of major phytohormones by scoring them as a module (Supporting Information S2: Table S7). We found that the genes associated with auxin and cytokinin biosynthesis were mainly overrepresented in xylem and meristematic cells, while BR, jasmonic acid, and ABA were mainly enriched in epidermal and mesophyll cells (Figure 3a). Of note, the genes involved in gibberellin, strigolactone, and ethylene biosynthesis were highly enriched in most cell types, suggesting their universal role in shoot and stolon development (Figure 3a). We also observed that, except for strigolactone, gene sets of the hormone response were

overrepresented (Figure 3b), implying key roles of these phytohormones in the growth and development of both tissues.

SAMs, along with cotyledons, expanding leaves, and root tissues, are the primary sites of auxin biosynthesis. Thus, we investigated the expression pattern of the genes associated with auxin biosynthesis and response at the single-cell resolution. We found that most genes of auxin biosynthesis were highly expressed in stolon cells in a cell type-specific manner, such as *YUC5-3*, *AO1-6*, *AAO3-1* and *TAR2-3* (Supporting Information S1: Figure S11a). A set of auxin responsive factors (ARFs) was overrepresented in almost all cell types of the stolon, including *ARF11*, *ARF8-3*, *ARF4* and *ARF1* (Figure 3c). Among them, *StARF8* is hypothesized to act as an activator of tuberization (Kondhare et al. 2021), suggesting that the other ARF members may have a similar function in the development of the stolon and tuber. We also found that PIN family members were mainly expressed in the VCs, including the xylem and phloem, consistent with its reported role in auxin transport via the vascular tissues (Blilou et al. 2005; Gälweiler et al. 1998).

Moreover, the genes involved in gibberellin biosynthesis were mainly enriched in shoot cells, whereas the genes related to gibberellin catabolism were highly expressed in stolon cells (Supporting Information S1: Figure S11b). For instance, we found that the gibberellin biosynthesis gene *StGA20OX1* was specifically expressed in MCs of the shoot, consistent with its reported effect in the repression of tuberization (Carrera et al. 2000). In addition, the gibberellin catabolism gene *StGA20OX1* was reported to be highly enriched in three cell types of the stolon, which is consistent with its important role in the early stages of tuber development in potato (Kloosterman et al. 2007). This expression pattern implies that the stolon may have a lower GA level compared to that of the shoot, which contributes to further tuber formation. The gibberellin-responsive genes were among the most divergent genes exhibiting a cell type-specific expression pattern (Supporting Information S1: Figure S11c). For example, the negative regulator of gibberellin *GAI-3* was highly expressed in four cell types of the stolon, including ECs, MEs, MCs, and PCs (Peng et al. 1997). *StSOC1* showed expression dominance in VCs and MCs of the stolon; its homologous gene in Arabidopsis, *AtSOC1*, is known to regulate the flowering time via gibberellin-dependent pathway, implying the potential role of *StSOC1* in stolon development (Moon et al. 2003). Another gibberellin-responsive gene, *GASA4*, was enriched in PCs of the stolon, consistent with induction of its homolog *AtGASA4* by gibberellin to promote the expression of gibberellin 20-oxidase in the *gasa4* Arabidopsis mutant (Rubinovich and Weiss 2010). Taken together, these results indicate that phytohormones, especially auxin and gibberellin, play an important role in shoot and stolon apical development in a cell type-specific manner (Roumeliotis, Kloosterman, et al. 2012; Salam et al. 2021; Xu et al. 1998).

FIGURE 2 | Transcriptional divergence between shoot and stolon cells. (a) and (b) UMAP visualization based on samples and cell clusters, respectively. (c) Correlation coefficients between the shoot and stolon for individual cell types. (d) Distribution of tissues-specific genes and conserved genes among cell types. (e) Heatmap plot of conserved genes among cell types. (f) Examples of two conserved genes, PDF1-3 and APL, with UMAP visualization. (g) Examples of tissue-specific genes with UMAP visualization. (h) Relative expression of the genes in (g). (i) Expression pattern of the target genes of *HY5* and PIF among cell types. EC, epidermal cell; ME, mesophyll cell; MC, meristem cell; PC, proliferating cell; XY, xylem; PH, phloem; VC^{P-X}, vascular cells excluding the phloem and xylem. [Color figure can be viewed at wileyonlinelibrary.com]

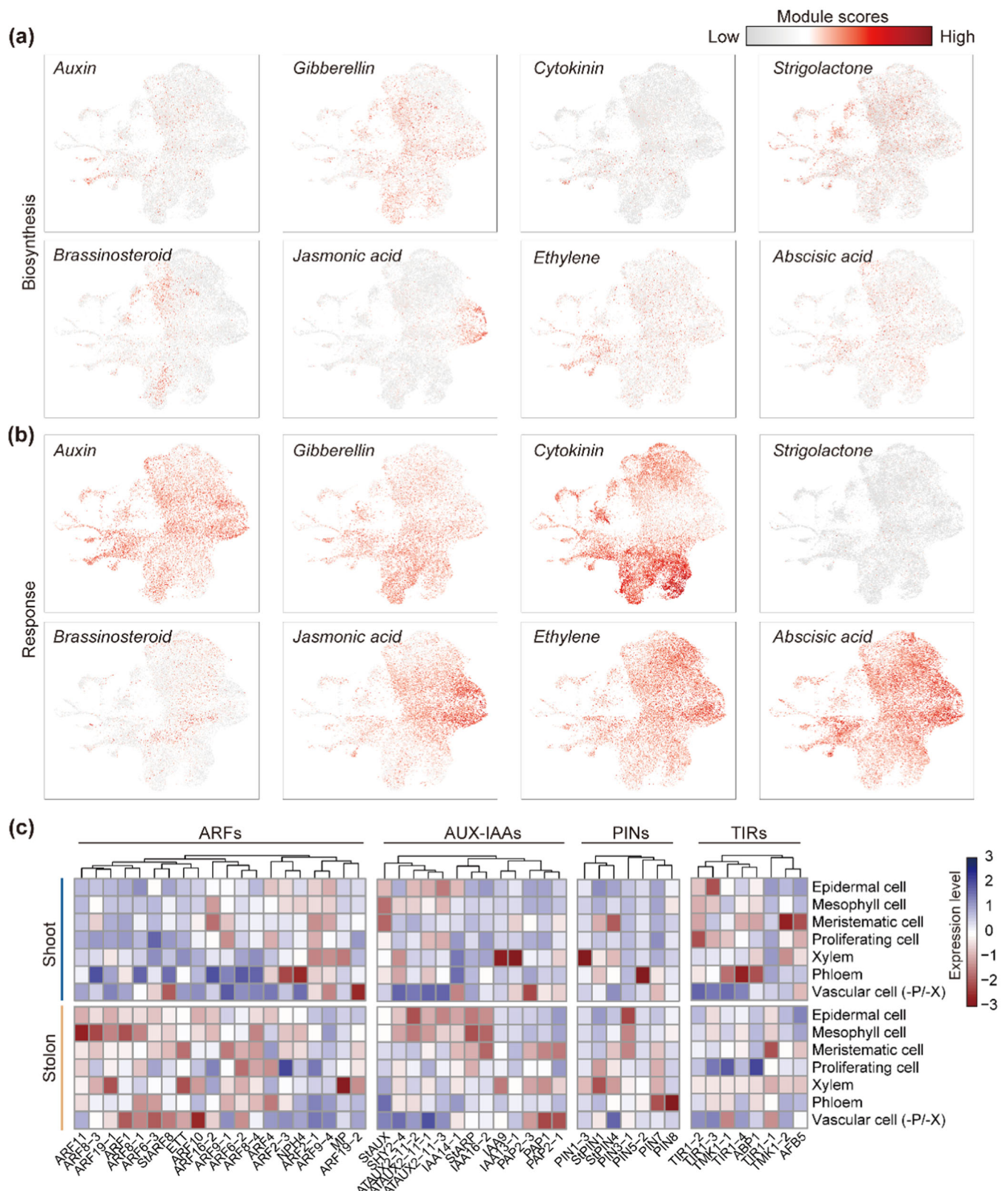


FIGURE 3 | UMAP visualization of expression patterns of genes related to hormones biosynthesis and responses. (a) and (b) Expression pattern of the gene sets related to hormones biosynthesis and responses, respectively. Eight hormones are shown, including auxin, gibberellin, cytokinin, strigolactone, brassinosteroid, jasmonic acid, ethylene, and abscisic acid. (c) Heatmap of expression patterns of genes related to auxin. [Color figure can be viewed at wileyonlinelibrary.com]

3.5 | Comparison of Meristematic Cells Between the Shoot and Stolon

As *STM* was reported to be highly expressed in the shoot apical meristems (SAMs) in *Arabidopsis* (Endrizzi et al. 1996), we compared the expression of *StPOTH15*, an ortholog of *STM* in *Arabidopsis*, in all cell types between the potato shoot and stolon. After filtering out the cells with no expression of *StPOTH15*, we found that the gene was more highly expressed and had a higher cell number in the stolon than in the shoot (Figure 4a), indicating higher meristematic capacity of the stolon. We named these cells with *StPOTH15* expression as differentiating *StPOTH15*-positive (*StPOTH15⁺*) cells, which were re-clustered into seven sub-clusters, named S0-S6. We found multiple marker genes of other cell types that were highly expressed among these sub-clusters, indicating an essential role of *StPOTH15* in the regulation of diverse developmental processes (Mahajan et al. 2016) (Figure 4b; Supporting Information S2: Table S8). For instance, cluster S0 contained several highly expressed phloem-related genes, such as *CALS3-2* and *ABS5-2*. The ME marker genes, such as *CAB1-1*, *BCB*, *FBA2-3* and *RBCS3B-1*, were predominantly expressed in S1. S3 was characterized by ECs based on high expression levels of the EC-specific genes *PDF1-1* and *FDH*. Subcluster S4 was assigned as the CCs, as revealed by enrichment of the CC-specific genes *TET6* and *EFM-2*. The xylem lineage genes *ACL5-3* and *PXY-1* were overrepresented in subcluster S5, which was considered to represent the xylem. The PC marker genes, including *FZR3*, *SYP111* and *3xHMG-box 2-1*, were highly enriched in subcluster S6. The subcluster S2 in the centre of the t-distributed stochastic neighbour embedding (tSNE) map was considered to represent pluripotent stem cells, which was supported by the high expression levels of *StPOTH15* and *StPOTH1* (Figure 4c). These results demonstrated the cell heterogeneity and differentiation lineages of the meristematic cells in potato.

By profiling subcluster S2, we identified a set of genes known to be related to the meristem, such as *LONESOME HIGHWAY* (*LHW-2*), *TYROSYLPROTEIN SULFOTRANSFERASE* (*TPST*), *TED4*, and *StPOTH15*, in both of the shoot and stolon (Figure 4d). We also identified 562 genes with upregulated expression in stolon cells compared to shoot cells, including several genes known to be involved in root formation. For instance, the expression of *KNAT6-1*, which is required for lateral root formation in *Arabidopsis*, was upregulated by 1.89-fold in stolon stem cells. The regulation of *UBP12/UBP13* on the *RGF1* receptor has been reported as a critical factor for root meristematic maintenance in *Arabidopsis* (An et al. 2018). The expression of *UBP12-2*, an ortholog of *UBP12*, in stolon stem cells was 2.52-fold higher than that in shoot stem cells. Moreover, genes related to sugar metabolism and shade avoidance, such as *UBC5-1* and *PHYA*, were dominant in stolon cells. In contrast, the shoot cells mainly exhibited high expression of genes related to photosynthesis. Function enrichment analysis showed that the upregulated genes in stolon cells were mainly associated with terms related to starch metabolism, mitochondria, and protein degradation, while the upregulated genes in shoot cells were mainly associated with photosynthesis and light responses functions (Figure 4e). We also observed diverse abiotic stress responses enriched in both the shoot and stolon cells, consisting of an endogenous stress-related signal for stem cell

maintenance (Zeng et al. 2021). These results indicated that starch metabolism may play a crucial role in the differentiation of shoot cells and stolon cells.

Notably, 6.2% (45) of the differentially expressed genes in sub-cluster S2 were TFs, exhibiting a tissue-specific dominant expression pattern across shoot and stolon MCs (Supporting Information S2: Table S9). Among the stolon-specific TFs, there were several genes related to development in *Arabidopsis* or rice, indicating that TFs play a key role in the determination of cell fate (Figure 4f). For instance, the TF *OsABF1* in rice, which is an abscisic acid (ABA)-responsive gene, can directly bind to the promoters of *Ehd1* and *Ehd2* to regulate flowering in rice (Tang et al. 2024). The *Arabidopsis* homeodomain-leucine zipper I (HD-Zip I) gene *AtHB1* was reported to be involved in leaf and hypocotyl development (Capella et al. 2015). *StMADS1*, also known as *POTM1-1*, is reported to be highly expressed in the axillary buds and underground stolon tips, suggesting a promoting role in the tuberization process of potato (Kang and Hannapel 1996; Kondhare et al. 2021). *Arabidopsis* MYB96 in the MYB TF family can regulate the accumulation of the MC marker gene *STM* to contribute to plant adaptation to environmental stress, such as drought stress (Lee et al. 2016).

We identified 72 and 39 TFs that were tightly co-expressed with *StPOTH15* in shoot and stolon stem cells, respectively (Supporting Information S2: Table S10). There were only four TFs co-expressed in shoot and stolon cells, including *ZFWD1*, *NF-YC1-4*, *NF-YC1-7* and *TIP1*. In shoot cells, the gene showing the strongest correlation with *StPOTH15* expression was *SCARECROW-LIKE 8* (*SCL8-1*, *Soltu.DM.03G018280*), which belongs to the family of *SCL* TFs that can regulate the downstream genes related to chlorophyll biosynthesis (Ma et al. 2014) (Figure 4g). The TF *LBD41-2*, a homolog of *LBD41* in *Arabidopsis*, has a potential role in shoot branching via interacting with *SCL6*, a key factor in meristem development (Smita et al. 2020). In *Arabidopsis*, overexpression of *EIN3* in transgenic plants resulted in enlarged SAMs and increased stem cell populations, whereas the *ein3-1eil2eil3* triple mutant showed reduced SAM sizes and stem cell pools (Zeng et al. 2021). Likewise, we observed that *EIN3-3* (*Soltu.DM.06G029100*) was the most strongly co-expressed TF with *StPOTH15* in stolon MCs, indicating that ethylene may participate in the maintenance of stolon cells in potato. In addition, the homologs of other regulators have been reported to play a role in regulation of meristem, such as *BPC6*, *SVP*, *BZIP29-1* and *GAI* (Dill and Sun 2001; Ehlers et al. 2016; Gregis et al. 2013; Mu et al. 2017; Van Leene et al. 2016). To validate the regulation of these transcription factors on *StPOTH15*, we randomly selected eight genes for luciferase assay in tobacco leaves, containing five genes with strong activations on *StPOTH15* (Figure 4h-j; Supporting Information S1: Figure S12). For example, the LUC/REN ratio of *StSOC1* was 3.93-fold higher than that of the empty vector (EV), while the LUC/REN ratio of *StLBD41-2* increased by 2.55-fold than EV (Figure 4i,j). Moreover, the other transcription factors, such as *StNAC2-5*, *StHB22-1* and *StRAP2.4-1*, also showed strong activations (Supporting Information S1: Figure S12). We also observed that these regulators were overrepresented in terms related to ethylene signal pathway and transcription regulation (Supporting Information S1: Figure S13). However, the pattern was quite different in terms

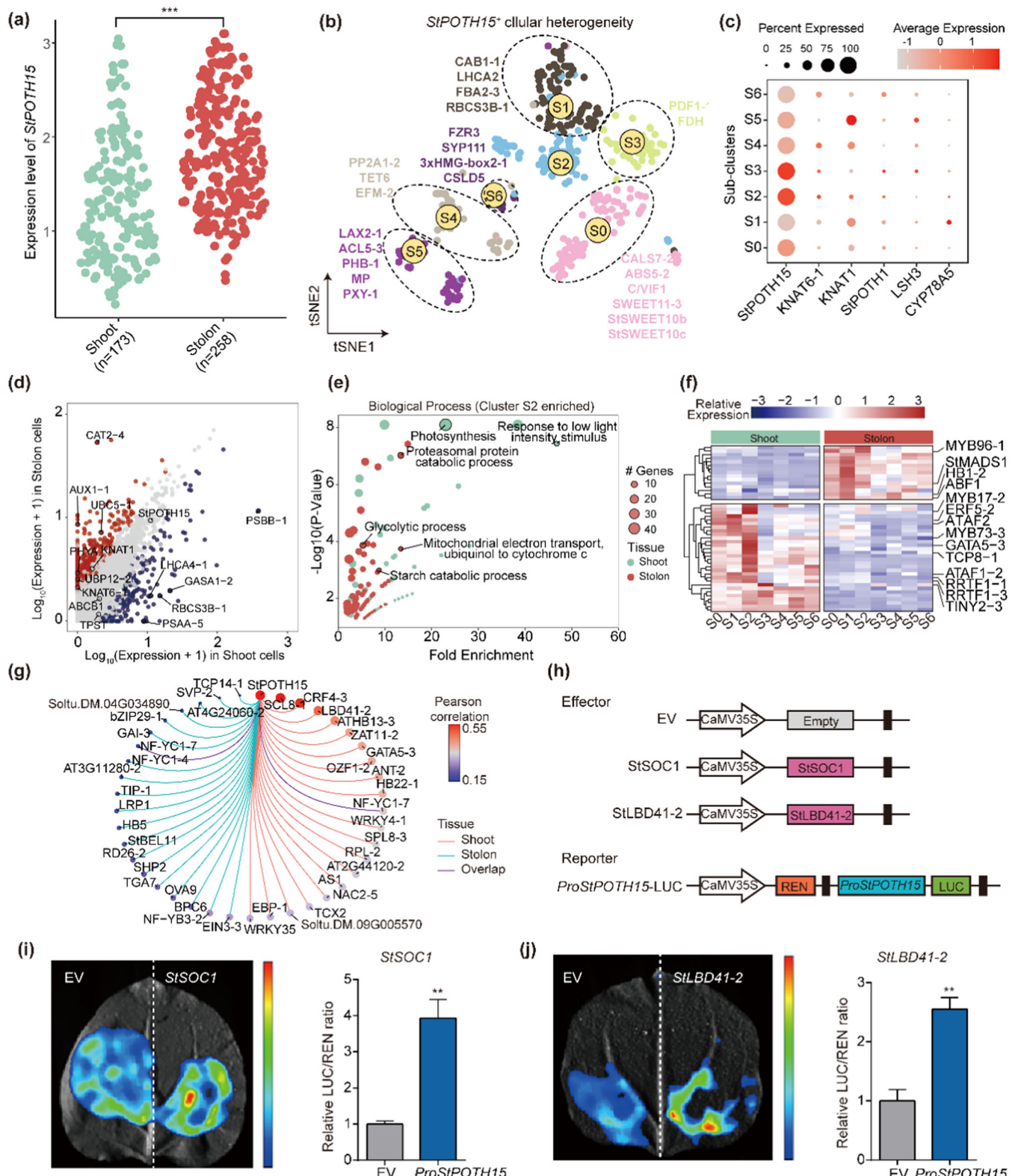


FIGURE 4 | Comparison of meristematic cells between the shoot and stolon. (a) Expression level difference of the cells expressing *StPOTH15* between the shoot and stolon. (b) Cell clustering of the *StPOTH15*⁺ cells. The representative marker genes for seven identified clusters are shown. (c) Expression pattern of *StPOTH15* among the seven clusters. (d) Volcano plot of genes in subcluster S2. The representative genes related to the meristem are shown. (e) GO enrichment results of the shoot-specific and stolon-specific genes in subcluster S2. (f) Heatmap of transcription factors in the tissue-specific genes. (g) Co-expression network between *StPOTH15* and transcription factors based on expression patterns in *StPOTH15*⁺ cells. (h) Vector construction for luciferase assay for the regulation on *StPOTH15*. (i) and (j) Representative activation of *StSOC1* (i) and *StLBD41-2* (j) on *StPOTH15*. Three replicates were conducted. Error bars represent the mean \pm SD of three biological triplicates. * p < 0.05 and ** p < 0.01 (Student's t test). [Color figure can be viewed at wileyonlinelibrary.com]

of phytohormones. For instance, the TFs co-expressed with *StPOTH15* in shoot MCs were enriched in terms related to cytokinin, while the co-expressed TFs in stolon MCs were more concentrated in terms related to auxin and gibberellin. In summary, these results revealed both common and specific regulatory mechanisms of cell differentiation between shoot and stolon meristematic cells, as highlighted by the collaboration of phytohormones and TFs.

3.6 | Differentiation Trajectory of Xylem-Related Cells

As we know, StSP6A, the homolog of FT in potato, functions as tuberigen to participate in the tuberization, which was expressed in leaves and transmitted through the phloem from the shoot apex to the stolon tips. Among this process, several genes which were specifically expressed in vascular cells cooperated with StSP6A to influence tuberization. Thus, characterizing the development of vascular tissues is crucial for investigating the mechanism of tuberization in potato. First, we focused on the developmental trajectory of the xylem cells. To investigate the detailed sub-clusters related to the xylem, we re-clustered the cells associated with xylem (cluster 14) into four sub-clusters, with subcluster X3 separated into other clusters (Figure 5a). According to the annotated marker genes, we defined subcluster X0 as the procambial region, with expression of the representative marker gene *WOX4* (*Soltu.DM.04G033400*). In particular, genes associated with tracheary elements, such as *XYLEM CYSTEINE PEPTIDASE 1* (*XCP1-1*, *Soltu.DM.04G037940*), were highly expressed in subcluster X4, which was considered to be a tracheary element cluster. Using Monocle3, cluster X0 characterized by high *WOX4* expression was set as the start site to obtain a single developed path, named I°-II° (Figure 5b).

We identified differences between the shoot and stolon cells along this trajectory reflecting development of the xylem. For instance, the shoot had a higher proportion of cells and higher expression levels than the stolon. However, the stolon had more cells with a lower pseudotime value during the early development stages than the shoot, pointing to the high developmental potentials in the stolon (Figure 5c). This developmental path was further supported by the dynamic expression of *WOX4*, *MP* and *XCP1* in these cells (Figure 5d). Integration of the dynamic expression and co-expression patterns showed that these genes formed four groups, named a, b, c and d, respectively (Figure 5e; Supporting Information S2: Table S11). Groups a and b were located at the start and middle parts of the pseudotime trajectory, including genes enriched in GO terms related to basic biological and cellular functions, such as ‘photosynthesis’, ‘transport’, ‘translation’ and ‘protein folding’ (Figure 5f). These results were in line with the active differentiation potential at this stage. Group ‘c’ represented the middle to late stages of development, including genes related to ‘xyloglucan metabolic process’, ‘cell wall biogenesis’ and ‘trehalose biosynthetic process’. However, group ‘d’ represented the terminal stage of development, which was enriched in genes related to ‘small GTPase mediated signal transduction’, ‘intracellular protein transport’, ‘microtubule-based process’ and ‘microtubule nucleation’, indicating a potential role in the transport of tracheary elements.

3.7 | Trajectory Analysis of Phloem-Originated Cells

We further investigated the trajectory of the phloem-originated cells by re-clustering the phloem cluster (cluster 16), grouping these cells into six sub-clusters. Using Monocle3, we obtained two distinct differentiated paths, named I°-III° and I°-IV°, respectively (Figure 6a). According to known phloem marker genes, we defined cluster 5 as the start site, characterized by high expression of cell cycle genes, such as *CYCA1;1-2* (*Soltu.DM.11G009620*). The auxin-related gene *AUX1-1* (*Soltu.DM.09G000480*) was also highly expressed among most cells, implying the potential role of auxin in phloem development. The sieve element-specific gene *SEOR1-2* (*Soltu.DM.05G010240*) was highly expressed in cluster P1, whereas *PP2A1-2* (*Soltu.DM.02G011940*), a CC-specific gene was highly expressed in cluster P3 (Figure 6b). Thus, we defined the paths ‘I°-III°’ and ‘I°-IV°’ as the CC and sieve element developmental path, respectively.

Comparison of the phloem expression data showed that the stolon had more cells than the shoot, especially in cluster P5 comprising multiple cell cycle-related genes (Figure 6c). The distribution of pseudotime values showed no obvious difference, with predominant expression in the late stage of development (Figure 6d). Gene modules analysis classified these development-related genes into three groups (Figure 6e; Supporting Information S2: Table S12). According to their expression patterns, group ‘b’ represented the start site with high expression in clusters P2 and P5; group ‘a’ was located at the terminal part of the CC developmental path (I°-III°); and group ‘c’ mainly comprised genes with high expression in sieve element cells (Figure 6f). To obtain further insights into the potential roles of these genes in phloem development, we performed GO enrichment analysis of biological processes on the gene modules (Figure 6g). As expected, the genes in group b were mainly associated with ‘translation’, ‘protein refolding’, ‘DNA replication’ and ‘translational elongation’, implying that these cells are in a highly active state. We also found that the genes in group ‘a’ were mainly enriched in the terms ‘intracellular protein transport’, ‘proteolysis involved in cellular protein catabolic process’, ‘vesicle-mediated transport’ and ‘small GTPase mediated -based process’. Likewise, the genes from group ‘c’ represented the potential transport function of sieve element cells with enrichment in terms associated with ‘photosynthesis’, ‘carboxylic acid metabolic process’ and ‘glucose metabolic process’, implying a role in sieve element transport photosynthesis.

3.8 | Consensus of Cell Types Between *Arabidopsis* and Potato

To dissect the transcriptional conservation and divergence of shoot development between species, we first calculated inter-species similarities among all cell types of the shoot apex scRNA-seq datasets from *Arabidopsis* and potato through MetaNeighbor analysis, which is based on a machine learning method to test the reproducibility of cell types between different datasets (Crow et al. 2018). Notably, almost all VCs, including the xylem, phloem, and CCs, showed high MetaNeighbor scores, suggesting

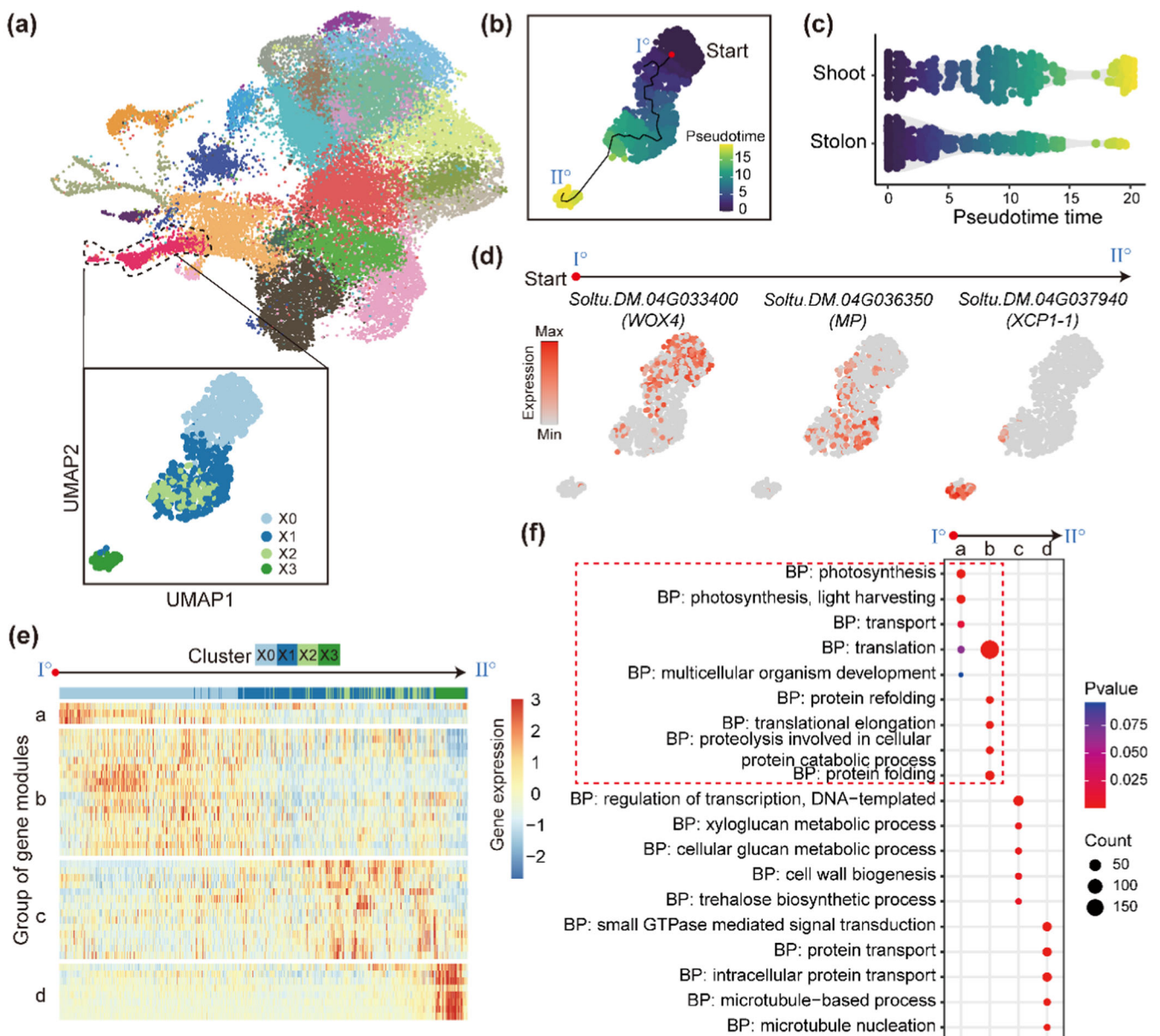


FIGURE 5 | Differentiation trajectory of xylem cells. (a) UMAP visualization of cell clustering on xylem cells with four sub-clusters, named X0, X1, X2, and X3. (b) Trajectory analysis on xylem cells by Monocle3 with the pseudotime path I°-II°. (c) Distribution of pseudotime values in shoot and stolon cells. (d) Trajectory path shown with three representative marker genes. (e) Expression kinetics of gene modules along the pseudotime paths of I°-II°, in which I° was considered to be the start site. The gene modules can be divided into four groups, labelled as 'a' to 'd'. Cells in these paths are shown along the pseudotime timeline and indicated by vertical lines with different cluster colour codes (cluster X0, cyan; cluster X1, blue; cluster X2, light green; cluster X3, dark green). (f) Top Gene Ontology (GO) terms of genes from each group. BP indicates biological process. [Color figure can be viewed at wileyonlinelibrary.com]

the conservation of vascular tissues between *Arabidopsis* and potato in both the shoot and stolon (Figure 7a). In addition, the ECs of the shoot in *Arabidopsis* showed high similarity with those of both the shoot and stolon of potato. However, the MEs of the shoot in *Arabidopsis* showed higher scores than those of the shoot but not those of the stolon cells in potato, supporting the divergence of MEs between the shoot and stolon across species. This similarity analysis was further supported by the shared markers between *Arabidopsis* and potato (Figure 7b).

We next explored the potential similarities between the stolon and root, which also grows underground. To address this question, we

collected public single-cell transcriptome datasets of the root tips of *Arabidopsis* and rice, and these data were integrated into a transcriptional landscape of root tissues in *Arabidopsis* and rice based on the single-copy homologous genes, respectively (Supporting Information S2: Table S13). The landscape of root cell types of *Arabidopsis* and rice were re-constructed with 20 and 14 clusters, respectively, based on known marker genes (Supporting Information S1: Figure S14). MetaNeighbor analysis for the comparison between potato and *Arabidopsis* or rice revealed that most cell types showed high similarities between species, which are restricted within different cell types from the same tissues. Only VCs of the potato shoot and stolon, such as the xylem and phloem, exhibited

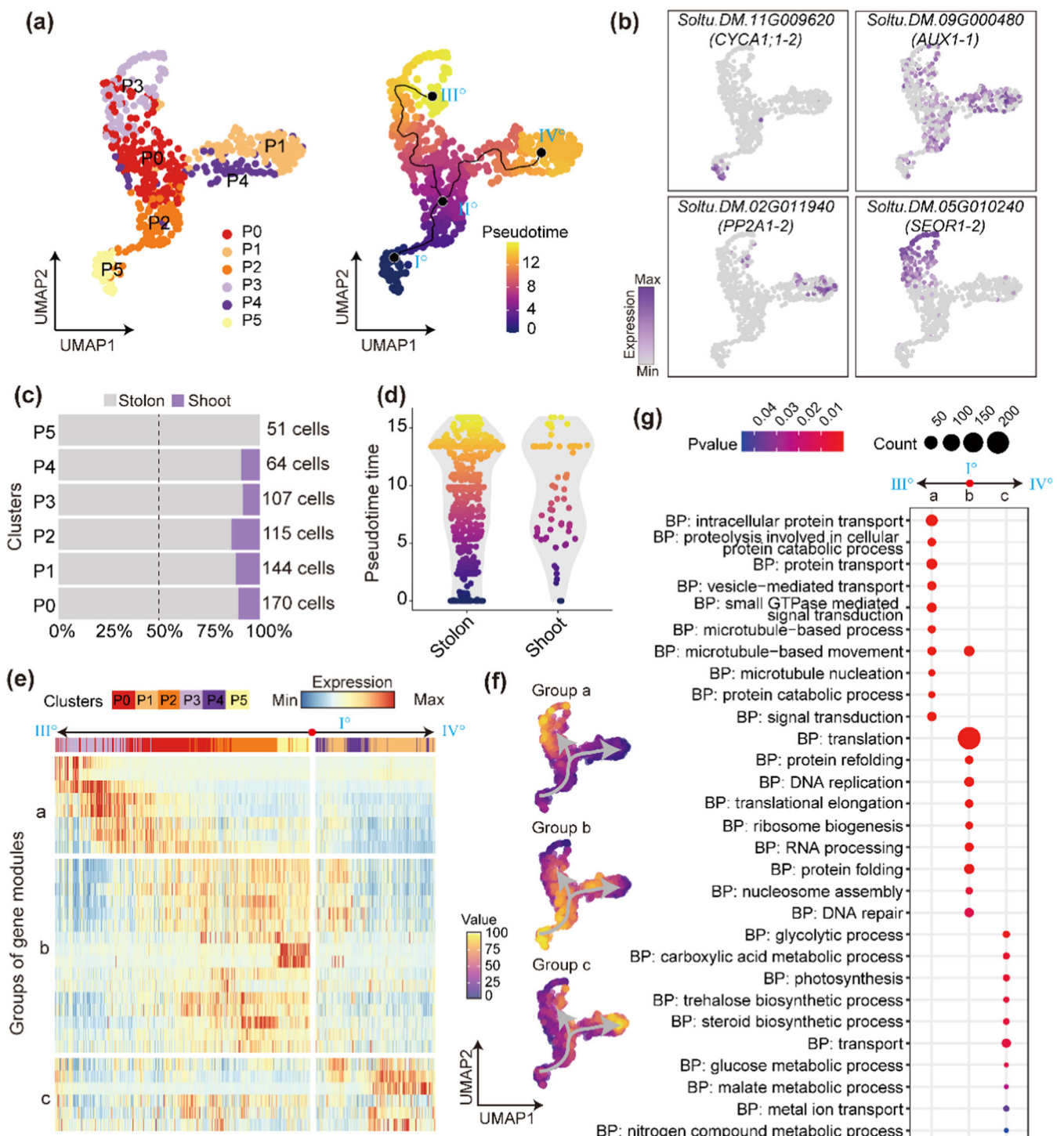


FIGURE 6 | Differentiation trajectory of phloem cells. (a) UMAP visualization of cell clustering on phloem cells; the left panel is the clustering on phloem cells and the right panel is the trajectory path of phloem cells. The trajectory can be determined as two paths, including I°-II°-III° and I°-II°-IV°. (b) UMAP visualization of representative marker genes. (c) Proportion of cells between different tissues. (d) Distribution of pseudotime value in shoot and stolon cells. (e) Expression kinetics of gene modules along the pseudotime paths of I°-II°-III° and I°-II°-IV°, reflecting the development of companion cells (CC) and the development of sieve elements (SE), respectively. The gene modules can be divided into three groups, labelled as 'a' to 'c'. Cells in these paths are shown bi-directionally along the pseudotime timeline and indicated by vertical lines with different cluster colour codes. (f) UMAP visualization of pseudotime value in different groups. (g) Top Gene Ontology (GO) terms of genes from each group. BP indicates biological process. [Color figure can be viewed at wileyonlinelibrary.com]

high reproducibility with the root tissues from Arabidopsis and rice, respectively (Supporting Information S1: Figure S15a and S15b). These results suggested that the stolon exhibited more transcriptional similarity with the shoot apex than with the root tissues.

To further dissect the divergence of the shoot apex between Arabidopsis and potato in a single-cell-specific manner, we conducted a combined analysis of single-cell transcriptome data from the shoot apex in Arabidopsis and potato, revealing 18

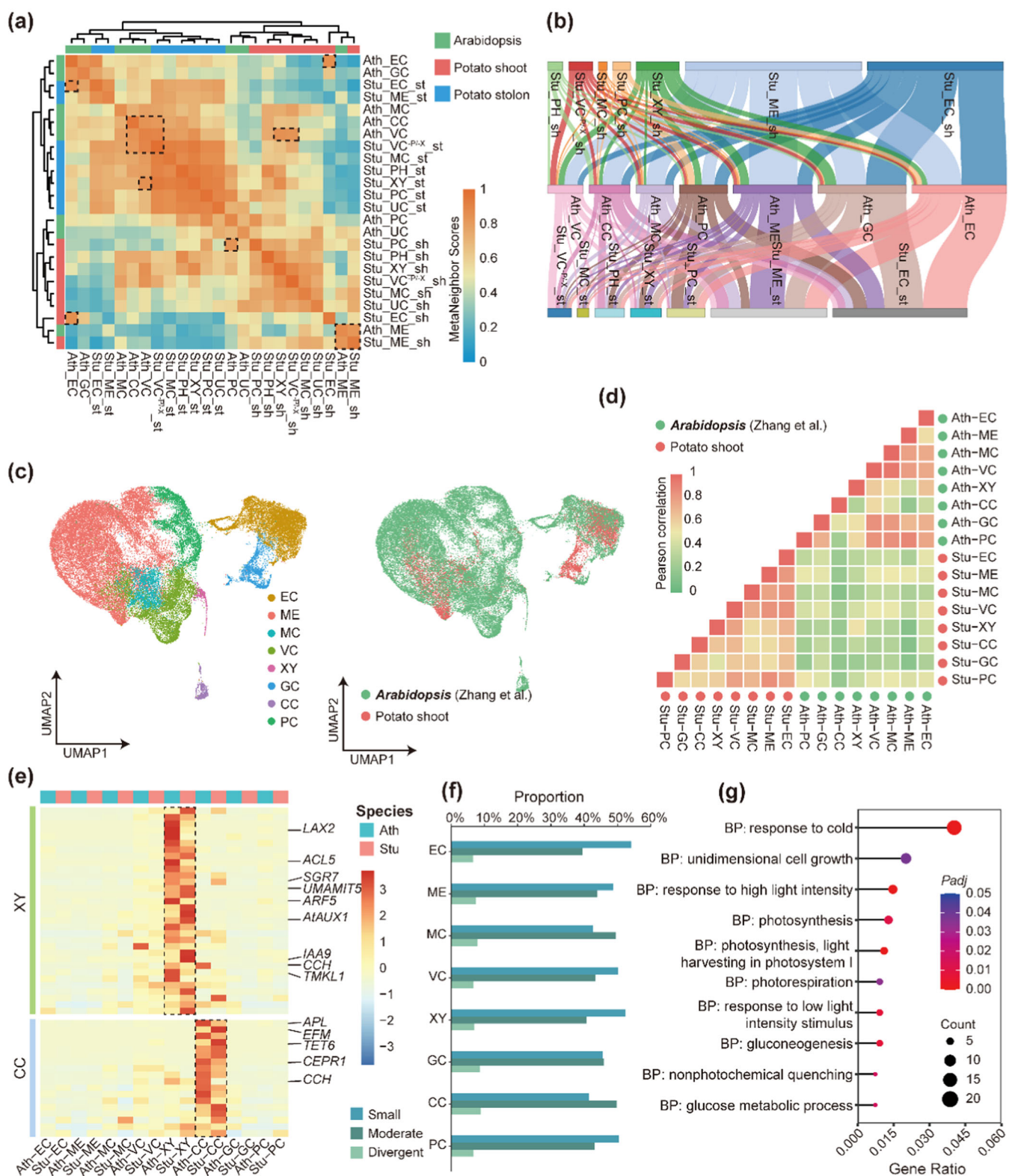


FIGURE 7 | Cross-species analysis between potato and Arabidopsis at the single-cell level. (a) MetaNeighbor analysis showing the similarities represented by the MetaNeighbor scores between cell types in the potato shoot apex and stolon tip and the Arabidopsis shoot apex. The colour represents MetaNeighbor scores. (b) Sankey plots of overlaps in marker genes between the potato shoot apex and stolon tip and the Arabidopsis shoot apex. (c) UMAP visualization of the integrated shoot apex datasets of potato and Arabidopsis. (d) Pearson correlation coefficients of expression levels in different cell types between potato and Arabidopsis. (e) Heatmap of expression levels of conserved genes in xylem and companion cells. (f) Proportion of three types of genes in different cells, including slightly differentiated, moderately differentiated, and highly divergent genes. (g) Gene Ontology (GO) enrichment analysis on the divergent genes. CC, companion cell; EC, epidermal cell; GC, guard cell; MC, meristem cell; ME, mesophyll cell; PC, proliferating cell; Sh, shoot; St, Stolon; VC, vascular cell; XY, xylem. [Color figure can be viewed at wileyonlinelibrary.com]

clusters with 66 407 cells and 6515 single-copy ortholog genes (Supporting Information S1: Figure S16a–b and Supporting Information S2: Table S13). According to known marker genes, seven representative cell types were covered, such as ECs, MEs, MCs, VCs, xylem cells, GCs, CCs, and PCs (Supporting Information S1: Figure S16c). Most ECs, MEs, GCs, and CCs in potato overlapped with the corresponding cells of Arabidopsis (Figure 7c). Of note, these cells shared high PCC values between the two species based on the gene expression levels (Figure 7d). Using VCs for further identification of conserved genes, a set of previously genes reported to be associated with the xylem and CCs showed high expression in both cell types in both species, including *LAX2*, *ACL5*, *ARF5* and *CCH* associated with xylem development and *APL*, *EFM*, *TET6* and *CEPR1* in CCs (Figure 7e).

Finally, we quantified the transcriptional changes of genes expressed in all cell types in the two species. ECs, the xylem, and PCs showed a higher number of genes with slight differences in expression levels and a lower number of divergent genes between species than other cell types, which may reflect the partially conserved function of these cells (Figure 7f; Supporting Information S1: Figure S12; Supporting Information S2: Table S14). In contrast, MEs, GCs, and CCs displayed more divergent genes, which may contribute to anatomical differences between Arabidopsis and potato. The top enriched GO terms of the divergent genes for each cell type were related to basic biological processes, such as ‘response to high light intensity’, ‘photosynthesis, light harvesting in photosystem I’ and ‘photorespiration’ (Figure 7f; Supporting Information S2: Table S15). The term ‘response to cold’ may be related to the difference in adaptations between species. Of note, these divergent genes were enriched in several terms related to sucrose metabolism, including ‘gluconeogenesis’ and ‘glucose metabolic process’, suggesting that these processes underlie the greatest difference between potato and Arabidopsis.

4 | Discussion

Potato is a representative plant species characterized by a modified stem known as the stolon, which can further grow into tubers comprising high amounts of water and carbohydrates as well as varying levels of proteins and vitamins. With the development of sequencing technologies, scRNA-seq has become increasingly popular in the field of developmental biology and has been applied to research on diverse plant species, including Arabidopsis, rice, wheat, soybean, maize, and poplar (Chen et al. 2021; Han et al. 2023; Z. Liu et al. 2023; Shahani et al. 2022; L. Zhang, Chen, and Wang et al. 2023). Although the molecular profiles of various cell types in the root apical meristem have been comprehensively determined for most of these plant species, especially Arabidopsis, the molecular characterization of cell types in the shoot apex and stolon tips remains largely incomplete. A recent scRNA-seq analysis of the shoot apex in Arabidopsis identified seven major cell types, providing a comprehensive landscape for further research on the shoot apex (T. Q. Zhang, Chen, and Wang 2021). Here, we conducted scRNA-seq on the shoot apex and stolon tips of potato, obtaining 23 cell clusters on 35 048 high-quality cells, which were classified into five major types based on the

homolog genes of the cell type-specific marker genes in *Arabidopsis* (Figure 1a,b). Our study thus provides the first transcriptome data set facilitating further investigations of the molecular mechanism of development of the shoot apex and stolon tips of potato at the single-cell level. Our results further provide numerous cell type-specific marker genes for additional functional studies on potato developmental biology, which is expected to accelerate the identification of cell types in the genus *Solanum*.

There is a fundamental gap in knowledge of potato development, which is largely based on a lack of understanding of the molecular differences in stem cells between the shoot apex and stolon tips as well as the link between transcription regulation and cell fate across the two tissues. Although several previous studies have explored the effects of diverse treatments on the development of the stolon and shoot, the detailed processes involved in cell fate determination and pattern formation in potato stem cells are poorly understood. In strawberries, the cell fate of the axillary buds was found to be dictated by a combination of environmental cues and endogenous signals, such as light and temperature (Andrés et al. 2021). Our scRNA-seq data revealed that the divergence in the pathways related to photosynthesis and phytohormones is mainly responsible for the morphological differences between the shoot apex and stolon tips of potato when comparing the two tissues at the single-cell levels (Figure 4). This finding is consistent with the hypothesis that the cell fate of the stolon apical meristems (STAMs) may be dictated by light perception, which triggers either tuberization or shoot formation (Kondhare et al. 2020). Previous studies have suggested that phytohormones play diverse roles in the development of potato, including stolon formation, stolon elongation, and tuberization (Abelenda and Prat 2013; Kloosterman et al. 2007; Rosin et al. 2003; Roumeliotis, Kloosterman, et al. 2012; Xu et al. 1998). Notably, gibberellins were considered to be the key phytohormone regulating development, acting as an inhibitor of stolon elongation, characterized by a decline in the expression level of a biosynthetic gene in parallel with the decline in the active gibberellin levels during stolon tip swelling and initiation of the tubers. Similar to gibberellin, the strigolactone acts as a repressor of axillary bud outgrowth and tuber formation. The content of auxin remains high at the early stages of development and then gradually decreases during the transition from a non-swelling to a swelling stolon and subsequent tuber formation (Roumeliotis, Kloosterman, et al. 2012; Roumeliotis, Visser, et al. 2012). In our data, we found higher expression of genes related to auxin in stolon cells, implying the promoting role of auxin in the non-swelling stage of the stolon (Figure 3). We also found divergent expression patterns of gibberellin-associated genes between the shoot and stolon cells of potato (Supporting Information S1: Figure S11). Compared to those of the shoot, the stolon displayed higher expression levels of gibberellin catabolism genes and lower expression levels of gibberellin biosynthesis genes, resulting in a lower bioactive gibberellin level in the stolon, which is favourable for tuber formation (Supporting Information S1: Figure S11b and S11c). We also observed enrichment of the BR response in both ECs and MEs, indicating a potential role of this hormone in the determination of cell fate between the shoot and stolon (Figure 3). Previous studies suggested that BR has a significant effect on meristematic cell growth and

division in both the shoot and the root (Hacham et al. 2011). However, the role of BR on the stolon remains unknown. Further studies on the application of BR and its inhibitor brassinazole or the establishment of knock-out mutants of BR biosynthetic genes may accelerate the investigation of the role of BR in stolon development. Moreover, the phytohormones showed dynamic expression during the stolon-to-tuber transition. Time series analysis of scRNA-seq in the stolon or whole tissues of potato along with establishment of a complete spatial transcriptome may contribute to elucidating the roles of phytohormones in the development of potato.

Two main mobile signals, StSP6A and StBEL5, are produced in the leaf and translocated via the vascular tissues to stimulate tuberization, highlighting the potential role of the vascular tissues in tuberization (Cho et al. 2015; Navarro et al. 2011). This long-distance process of transmitting signals from the leaves to the stolon motivated us to reconstruct the developmental trajectory of VCs, including the xylem and phloem (Figures 5 and 6). We identified numerous marker genes, which are homologs of the known VC-specific genes in Arabidopsis, that exhibited significant enrichment during the developmental process, indicating their conserved functions on the differentiation of vascular-related cells in potato. For example, *WOX4* (*Soltu.DM.04G033400*) was highly expressed in the early stage of xylem differentiation, which was consistent with its reported role in procambial development (Suer et al. 2011). A member of the SEOR1 family (*SEOR1-2*, *Soltu.DM.05G010240*) showed a specifically dominant expression pattern in the branch of sieve elements, indicating its involvement in the regulation of phloem transport and signalling (Knoblauch et al. 2014). A recent study showed that silencing the expression of *StSWEET11*, encoding a sugar transporter that binds to StSP6A to block sucrose leakage into the apoplast, downregulated the expression of StSP6A to ultimately decrease the number of tubers and tuber weight (Abelenda et al. 2019). This mediation effect on sucrose transport and unloading suggests a crucial role of the VCs in the tuber development in potato.

We further investigated the transcriptional divergence between potato and Arabidopsis or rice according to individual cell types, including the cells of the shoot apex and root tips. Cross-species analysis showed that VCs, including the xylem and phloem, exhibited highly conserved transcription patterns between potato and Arabidopsis (Figure 7a,b). Most of the marker genes of xylem and companion cells were conserved in the shoot apex between potato and Arabidopsis (Figure 7e). GO functional enrichment analysis showed that the divergent genes between species are mainly associated with the cold response, photosynthesis, and sugar metabolism, suggesting divergence in regulatory mechanisms during the evolution of these plants from the common ancestor (Figure 7g). These functional divergences of orthologous genes have thus contributed to plant evolution related to specific adaptations to diverse environments (Hegarty and Hiscock 2008; Z. Yang et al. 2015).

Acknowledgements

The computations in this paper were run on the π 2.0 cluster supported by the Center for High Performance Computing at Shanghai Jiao Tong

University. This research was supported by the National Natural Science Foundation of China (32071160, 32161133021), and Shanghai Collaborative Innovation Center of Agri-Seeds Foundation (ZXWH2150201/012).

Conflicts of Interest

The authors declare no conflicts of interest.

Data Availability Statement

The data that supports the findings of this study are available in the Supporting Information of this article.

References

- Abe, M., T. Takahashi, and Y. Komeda. 2001. "Identification of a Cis-Regulatory Element for L1 Layer-Specific Gene Expression, Which Is Targeted by an L1-specific Homeodomain Protein." *Plant Journal* 26, no. 5: 487–494.
- Abelenda, J. A., S. Bergonzi, M. Oortwijn, et al. 2019. "Source-Sink Regulation Is Mediated by Interaction of an FT Homolog With a SWEET Protein in Potato." *Current Biology* 29, no. 7: 1178–1186.e1176.
- Abelenda, J. A., and S. Prat. 2013. "Cytokinins: Determinants of Sink Storage Ability." *Current Biology* 23, no. 13: R561–R563. <https://doi.org/10.1016/j.cub.2013.05.020>.
- An, Z., Y. Liu, Y. Ou, et al. 2018. "Regulation of the Stability of RGF1 Receptor by the Ubiquitin-Specific Proteases UBP12/UBP13 Is Critical for Root Meristem Maintenance." *Proceedings of the National Academy of Sciences* 115, no. 5: 1123–1128. <https://doi.org/10.1073/pnas.1714177115>.
- Andrés, J., J. Caruana, J. Liang, et al. 2021. "Woodland Strawberry Axillary Bud Fate Is Dictated by a Crosstalk of Environmental and Endogenous Factors." *Plant Physiology* 187, no. 3: 1221–1234. <https://doi.org/10.1093/plphys/kiac421>.
- Blilou, I., J. Xu, M. Wildwater, et al. 2005. "The PIN Auxin Efflux Facilitator Network Controls Growth and Patterning in *Arabidopsis* Roots." *Nature* 433, no. 7021: 39–44. <https://doi.org/10.1038/nature03184>.
- Bonke, M., S. Thitamadee, A. P. Mähönen, M.-T. Hauser, and Y. Helariutta. 2003. "apl Regulates Vascular Tissue Identity in *Arabidopsis*." *Nature* 426, no. 6963: 181–186. <https://doi.org/10.1038/nature02100>.
- Bou-Torrent, J., J. F. Martínez-García, J. L. García-Martínez, and S. Prat. 2011. "Gibberellin A1 Metabolism Contributes to the Control of Photoperiod-Mediated Tuberization in Potato." *PLoS One* 6, no. 9: e24458. <https://doi.org/10.1371/journal.pone.0024458>.
- Capella, M., P. A. Ribone, A. L. Arce, and R. L. Chan. 2015. "*Arabidopsis thaliana* Homeobox 1 (AtHB1), a Homedomain-Leucine Zipper I (Hd-Zip I) Transcription Factor, Is Regulated by PHYTOCHROME-INTERACTING FACTOR to Promote Hypocotyl Elongation." *New Phytologist* 207, no. 3: 669–682.
- Carrera, E., J. Bou, J. L. García-Martínez, and S. Prat. 2000. "Changes in GA 20-Oxidase Gene Expression Strongly Affect Stem Length, Tuber Induction and Tuber Yield of Potato Plants." *Plant Journal* 22, no. 3: 247–256.
- Celis-gamboa, C., P. C. Struik, E. Jacobsen, and R. G. F. Visser. 2003. "Temporal Dynamics of Tuber Formation and Related Processes in a Crossing Population of Potato (*Solanum tuberosum*)."*Annals of Applied Biology* 143, no. 2: 175–186.
- Chen, Y., S. Tong, Y. Jiang, et al. 2021. "Transcriptional Landscape of Highly Lignified Poplar Stems at Single-Cell Resolution." *Genome Biology* 22, no. 1: 319. <https://doi.org/10.1186/s13059-021-02537-2>.
- Cho, S. K., P. Sharma, N. M. Butler, et al. 2015. "Polypyrimidine Tract-Binding Proteins of Potato Mediate Tuberization Through an

- Interaction With StBEL5 RNA." *Journal of Experimental Botany* 66, no. 21: 6835–6847. <https://doi.org/10.1093/jxb/erv389>.
- Crow, M., A. Paul, S. Ballouz, Z. J. Huang, and J. Gillis. 2018. "Characterizing the Replicability of Cell Types Defined by Single Cell RNA-Sequencing Data Using Metaneighbor." *Nature Communications* 9, no. 1: 884. <https://doi.org/10.1038/s41467-018-03282-0>.
- Denyer, T., X. Ma, S. Klesen, E. Scacchi, K. Nieselt, and M. C. P. Timmermans. 2019. "Spatiotemporal Developmental Trajectories in the *Arabidopsis* Root Revealed Using High-Throughput Single-Cell RNA Sequencing." *Developmental Cell* 48, no. 6: 840–852.e845.
- Dill, A., and T. Sun. 2001. "Synergistic Derepression of Gibberellin Signaling by Removing RGA and GAI Function in *Arabidopsis thaliana*." *Genetics* 159, no. 2: 777–785. <https://doi.org/10.1093/genetics/159.2.777>.
- Du, L., and B. W. Poovaiah. 2005. "Ca²⁺/calmodulin Is Critical for Brassinosteroid Biosynthesis and Plant Growth." *Nature* 437, no. 7059: 741–745. <https://doi.org/10.1038/nature03973>.
- Ehlers, K., A. S. Bhide, D. G. Tekleyohans, B. Wittkop, R. J. Snowdon, and A. Becker. 2016. "The MADS Box Genes Abs, SHP1, and SHP2 Are Essential for the Coordination of Cell Divisions in Ovule and Seed Coat Development and for Endosperm Formation in *Arabidopsis thaliana*." *PLoS One* 11, no. 10: e0165075. <https://doi.org/10.1371/journal.pone.0165075>.
- Emms, D. M., and S. Kelly. 2019. "OrthoFinder: Phylogenetic Orthology Inference for Comparative Genomics." *Genome Biology* 20, no. 1: 238. <https://doi.org/10.1186/s13059-019-1832-y>.
- Endrizzi, K., B. Moussian, A. Haecker, J. Z. Levin, and T. Laux. 1996. "The SHOOT MERISTEMLESS Gene Is Required for Maintenance of Undifferentiated Cells in *Arabidopsis* Shoot and Floral Meristems and Acts at a Different Regulatory Level Than the Meristem Genes *Wuschel* and *ZWILLE*." *Plant Journal* 10, no. 6: 967–979.
- Faivre-Rampant, O., L. Cardle, D. Marshall, R. Viola, and M. A. Taylor. 2004. "Changes in Gene Expression During Meristem Activation Processes in *Solanum tuberosum* With a Focus on the Regulation of an Auxin Response Factor Gene." *Journal of Experimental Botany* 55, no. 397: 613–622. <https://doi.org/10.1093/jxb/erh075>.
- Gangappa, S. N., and J. F. Botto. 2016. "The Multifaceted Roles of HY5 in Plant Growth and Development." *Molecular Plant* 9, no. 10: 1353–1365.
- Gälweiler, L., C. Guan, A. Müller, et al. 1998. "Regulation of Polar Auxin Transport by AtPIN1 in *Arabidopsis* Vascular Tissue." *Science* 282, no. 5397: 2226–2230. <https://doi.org/10.1126/science.282.5397.2226>.
- Ghate, T. H., P. Sharma, K. R. Kondhare, D. J. Hannapel, and A. K. Banerjee. 2017. "The Mobile RNAs, StBEL11 and StBEL29, Suppress Growth of Tubers in Potato." *Plant Molecular Biology* 93, no. 6: 563–578. <https://doi.org/10.1007/s11103-016-0582-4>.
- Gregis, V., F. Andrés, A. Sessa, et al. 2013. "Identification of Pathways Directly Regulated By SHORT VEGETATIVE PHASE During Vegetative and Reproductive Development in *Arabidopsis*." *Genome Biology* 14, no. 6: R56. <https://doi.org/10.1186/gb-2013-14-6-r56>.
- Hacham, Y., N. Holland, C. Butterfield, et al. 2011. "Brassinosteroid Perception in the Epidermis Controls Root Meristem Size." *Development* 138, no. 5: 839–848. <https://doi.org/10.1242/dev.061804>.
- Han, X., Y. Zhang, Z. Lou, et al. 2023. "Time Series Single-Cell Transcriptional Atlases Reveal Cell Fate Differentiation Driven by Light in *Arabidopsis* Seedlings." *Nature Plants* 9: 2095–2109. <https://doi.org/10.1038/s41477-023-01544-4>.
- Hartmann, A., M. Senning, P. Hedden, U. Sonnewald, and S. Sonnewald. 2011. "Reactivation of Meristem Activity and Sprout Growth in Potato Tubers Require Both Cytokinin and Gibberellin." *Plant Physiology* 155, no. 2: 776–796. <https://doi.org/10.1104/pp.110.168252>.
- Hastilestar, B. R., J. Lorenz, S. Reid, et al. 2018. "Deciphering Source and Sink Responses of Potato Plants (*Solanum tuberosum* L.) to Elevated Temperatures." *Plant, Cell & Environment* 41, no. 11: 2600–2616.
- Hegarty, M. J., and S. J. Hiscock. 2008. "Genomic Clues to the Evolutionary Success of Polyploid Plants." *Current Biology* 18, no. 10: R435–R444. <https://doi.org/10.1016/j.cub.2008.03.043>.
- Kang, S.-G., and D. J. Hannapel. 1996. "A Novel Mads-Box Gene of Potato (*Solanum tuberosum* L.) Expressed During the Early Stages of Tuberization." *Plant Molecular Biology* 31, no. 2: 379–386. <https://doi.org/10.1007/BF00021798>.
- Kloosterman, B., C. Navarro, G. Bijsterbosch, et al. 2007. "StGA2ox1 Is Induced Prior to Stolon Swelling and Controls Ga Levels During Potato Tuber Development." *Plant Journal* 52, no. 2: 362–373.
- Knoblauch, M., D. R. Froelich, W. F. Pickard, and W. S. Peters. 2014. "SEORious Business: Structural Proteins in Sieve Tubes and Their Involvement in Sieve Element Occlusion." *Journal of Experimental Botany* 65, no. 7: 1879–1893. <https://doi.org/10.1093/jxb/eru071>.
- Kolachevskaya, O. O., V. V. Alekseeva, L. I. Sergeeva, et al. 2015. "Expression of Auxin Synthesis Gene *tms1* Under Control of Tuber-Specific Promoter Enhances Potato Tuberization In Vitro." *Journal of Integrative Plant Biology* 57, no. 9: 734–744.
- Kondhare, K. R., A. Kumar, N. S. Patil, N. N. Malankar, K. Saha, and A. K. Banerjee. 2021. "Development of Aerial and Belowground Tubers in Potato Is Governed by Photoperiod and Epigenetic Mechanism." *Plant Physiology* 187, no. 3: 1071–1086. <https://doi.org/10.1093/plphys/kiab409>.
- Kondhare, K. R., B. Natarajan, and A. K. Banerjee. 2020. "Molecular Signals That Govern Tuber Development in Potato." *International Journal of Developmental Biology* 64, no. 1–2–3: 133–140. <https://doi.org/10.1387/ijdb.190132ab>.
- Korsunsky, I., N. Millard, J. Fan, et al. 2019. "Fast, Sensitive and Accurate Integration of Single-Cell Data With Harmony." *Nature Methods* 16, no. 12: 1289–1296. <https://doi.org/10.1038/s41592-019-0619-0>.
- Kumar, D., and P. F. Wareing. 1972. "Factors Controlling Stolon Development in the Potato Plant." *New Phytologist* 71, no. 4: 639–648.
- Lee, H. G., Y.-R. Choi, and P. J. Seo. 2016. "Increased STM Expression Is Associated With Drought Tolerance in *Arabidopsis*." *Journal of Plant Physiology* 201: 79–84.
- Van Leene, J., J. Blomme, S. R. Kulkarni, et al. 2016. "Functional Characterization of the *Arabidopsis* Transcription Factor bZIP29 Reveals Its Role in Leaf and Root Development." *Journal of Experimental Botany* 67, no. 19: 5825–5840. <https://doi.org/10.1093/jxb/erw347>.
- Lehretz, G. G., S. Sonnewald, C. Hornyik, J. M. Corral, and U. Sonnewald. 2019. "Post-Transcriptional Regulation of FLOWERING LOCUS T Modulates Heat-Dependent Source-Sink Development in Potato." *Current Biology* 29, no. 10: 1614–1624.e1613.
- Leivar, P., and P. H. Quail. 2011. "PIFs: Pivotal Components in a Cellular Signaling Hub." *Trends in Plant Science* 16, no. 1: 19–28.
- Li, C., S. Zhang, X. Yan, P. Cheng, and H. Yu. 2023. "Single-Nucleus Sequencing Deciphers Developmental Trajectories in Rice Pistils." *Developmental Cell* 58, no. 8: 694–708.e694.
- Liu, Q., Z. Liang, D. Feng, et al. 2021. "Transcriptional Landscape of Rice Roots at the Single-Cell Resolution." *Molecular Plant* 14, no. 3: 384–394. <https://doi.org/10.1016/j.molp.2020.12.014>.
- Liu, Z., X. Kong, Y. Long, et al. 2023. "Integrated Single-Nucleus and Spatial Transcriptomics Captures Transitional States in Soybean Nodule Maturation." *Nature Plants* 9, no. 4: 515–524. <https://doi.org/10.1038/s41477-023-01387-z>.
- Lü, S., H. Zhao, E. P. Parsons, et al. 2011. "The *glossyhead1* Allele of ACC1 Reveals a Principal Role for Multidomain Acetyl-Coenzyme A

- Carboxylase in the Biosynthesis of Cuticular Waxes by Arabidopsis." *Plant Physiology* 157, no. 3: 1079–1092. <https://doi.org/10.1104/pp.111.185132>.
- Ma, Z., X. Hu, W. Cai, et al. 2014. "Arabidopsis miR171-Targeted Scarecrow-Like Proteins Bind to GT cis-Elements and Mediate Gibberellin-Regulated Chlorophyll Biosynthesis Under Light Conditions." *PLoS Genetics* 10, no. 8: e1004519. <https://doi.org/10.1371/journal.pgen.1004519>.
- Mahajan, A. S., K. R. Kondhare, M. P. Rajabhoj, et al. 2016. "Regulation, Overexpression, and Target Gene Identification of Potato Homeobox 15 (POTH15)—A Class-I KNOX Gene in Potato." *Journal of Experimental Botany* 67, no. 14: 4255–4272. <https://doi.org/10.1093/jxb/erw205>.
- Marand, A. P., Z. Chen, A. Gallavotti, and R. J. Schmitz. 2021. "A Cis-Regulatory Atlas in Maize at Single-Cell Resolution." *Cell* 184, no. 11: 3041–3055.e3021. <https://doi.org/10.1016/j.cell.2021.04.014>.
- McGinnis, C. S., L. M. Murrow, and Z. J. Gartner. 2019. "DoubletFinder: Doublet Detection in Single-Cell RNA Sequencing Data Using Artificial Nearest Neighbors." *Cell Systems* 8, no. 4: 329–337.e324.
- Moon, J., S.-S. Suh, H. Lee, et al. 2003. "The SOC1 MADS-Box Gene Integrates Vernalization and Gibberellin Signals for Flowering in Arabidopsis." *Plant Journal* 35, no. 5: 613–623.
- Mu, Y., M. Zou, X. Sun, et al. 2017. "Basic Pentacysteine Proteins Repress ABSCISIC ACID INSENSITIVE4 Expression via Direct Recruitment of the Polycomb-Repressive Complex 2 in Arabidopsis Root Development." *Plant & Cell Physiology* 58, no. 3: 607–621. <https://doi.org/10.1093/pcp/pcx006>.
- Navarro, C., J. A. Abelenda, E. Cruz-Oró, et al. 2011. "Control of Flowering and Storage Organ Formation in Potato by FLOWERING LOCUS T." *Nature* 478, no. 7367: 119–122. <https://doi.org/10.1038/nature10431>.
- Nguyen, T. H., L. Thiers, A. Van Moerkercke, et al. 2023. "A Redundant Transcription Factor Network Steers Spatiotemporal Arabidopsis Triterpene Synthesis." *Nature Plants* 9: 926–937. <https://doi.org/10.1038/s41477-023-01419-8>.
- Nicolas, M., R. Torres-Pérez, V. Wahl, et al. 2022. "Spatial Control of Potato Tuberization by the TCP Transcription Factor BRANCHED1b." *Nature Plants* 8, no. 3: 281–294. <https://doi.org/10.1038/s41477-022-01112-2>.
- Nolan, T. M., N. Vukašinović, C.-W. Hsu, et al. 2023. "Brassinosteroid Gene Regulatory Networks at Cellular Resolution in the Arabidopsis Root." *Science* 379, no. 6639: eadf4721. <https://doi.org/10.1126/science.adf4721>.
- Park, J.-S., S.-J. Park, S.-Y. Kwon, et al. 2022. "Temporally Distinct Regulatory Pathways Coordinate Thermo-Responsive Storage Organ Formation in Potato." *Cell Reports* 38, no. 13: 110579.
- Pasare, S. A., L. J. M. Dureux, W. L. Morris, et al. 2013. "The Role of the Potato (*Solanum tuberosum*) CCD8 Gene in Stolon and Tuber Development." *New Phytologist* 198, no. 4: 1108–1120.
- Peng, J., P. Carol, D. E. Richards, et al. 1997. "The Arabidopsis Gai Gene Defines a Signaling Pathway That Negatively Regulates Gibberellin Responses." *Genes & Development* 11, no. 23: 3194–3205. <https://doi.org/10.1101/gad.11.23.3194>.
- Rosin, F. M., J. K. Hart, H. T. Horner, P. J. Davies, and D. J. Hannapel. 2003. "Overexpression of a Knotted-Like Homeobox Gene of Potato Alters Vegetative Development by Decreasing Gibberellin Accumulation." *Plant Physiology* 132, no. 1: 106–117. <https://doi.org/10.1104/pp.102.015560>.
- Roumeliotis, E., B. Kloosterman, M. Oortwijn, et al. 2012. "The Effects of Auxin and Strigolactones on Tuber Initiation and Stolon Architecture in Potato." *Journal of Experimental Botany* 63, no. 12: 4539–4547. <https://doi.org/10.1093/jxb/ers132>.
- Roumeliotis, E., B. Kloosterman, M. Oortwijn, T. Lange, R. G. F. Visser, and C. W. B. Bachem. 2013. "Down Regulation of StGA3ox Genes in Potato Results in Altered GA Content and Affect Plant and Tuber Growth Characteristics." *Journal of Plant Physiology* 170, no. 14: 1228–1234.
- Roumeliotis, E., R. G. F. Visser, and C. W. B. Bachem. 2012. "A Crosstalk of Auxin and GA During Tuber Development." *Plant Signaling & Behavior* 7, no. 10: 1360–1363. <https://doi.org/10.4161/psb.21515>.
- Rubinovich, L., and D. Weiss. 2010. "The Arabidopsis Cysteine-Rich Protein GASA4 Promotes GA Responses and Exhibits Redox Activity in Bacteria and in *Planta*." *Plant Journal* 64, no. 6: 1018–1027.
- Ryu, K. H., L. Huang, H. M. Kang, and J. Schiefelbein. 2019. "Single-Cell RNA Sequencing Resolves Molecular Relationships Among Individual Plant Cells." *Plant Physiology* 179, no. 4: 1444–1456. <https://doi.org/10.1104/pp.18.01482>.
- Salam, B. B., F. Barbier, R. Danieli, et al. 2021. "Sucrose Promotes Stem Branching Through Cytokinin." *Plant Physiology* 185, no. 4: 1708–1721. <https://doi.org/10.1093/plphys/kiab003>.
- Satija, R., J. A. Farrell, D. Gennert, A. F. Schier, and A. Regev. 2015. "Spatial Reconstruction of Single-Cell Gene Expression Data." *Nature Biotechnology* 33, no. 5: 495–502. <https://doi.org/10.1038/nbt.3192>.
- Satterlee, J. W., L. J. Evans, B. R. Conlon, et al. 2023. "A Wox3-Patterning Module Organizes Planar Growth in Grass Leaves and Ligules." *Nature Plants* 9, no. 5: 720–732. <https://doi.org/10.1038/s41477-023-01405-0>.
- Satterlee, J. W., J. Strable, and M. J. Scanlon. 2020. "Plant Stem-Cell Organization and Differentiation at Single-Cell Resolution." *Proceedings of the National Academy of Sciences* 117, no. 52: 33689–33699. <https://doi.org/10.1073/pnas.2018788117>.
- Shahan, R., C. W. Hsu, T. M. Nolan, et al. 2022. "A Single-Cell Arabidopsis Root Atlas Reveals Developmental Trajectories in Wild-Type and Cell Identity Mutants." *Developmental Cell* 57, no. 4: 543–560.e549. <https://doi.org/10.1016/j.devcel.2022.01.008>.
- Smita, S., J. Kiehne, S. Adhikari, E. Zeng, Q. Ma, and S. Subramanian. 2020. "Gene Regulatory Networks Associated With Lateral Root and Nodule Development in Soybean." *In silico Plants* 2, no. 1: diaa002. <https://doi.org/10.1093/insilicoplants/diaa002>.
- Struik, P. C. 2007. "Chapter 11—Above-Ground and Below-Ground Plant Development." In *Potato Biology and Biotechnology*, edited by D. Vreugdenhil, J. Bradshaw, C. Gebhardt, et al., 219–236. Elsevier Science B.V.
- Suer, S., J. Agusti, P. Sanchez, M. Schwarz, and T. Greb. 2011. "WOX4 Imparts Auxin Responsiveness to Cambium Cells in Arabidopsis." *Plant Cell* 23, no. 9: 3247–3259. <https://doi.org/10.1105/tpc.111.087874>.
- Sun, X., D. Feng, M. Liu, et al. 2022. "Single-Cell Transcriptome Reveals Dominant Subgenome Expression and Transcriptional Response to Heat Stress in Chinese Cabbage." *Genome Biology* 23, no. 1: 262. <https://doi.org/10.1186/s13059-022-02834-4>.
- Sun, Y., Y. Han, K. Sheng, et al. 2023. "Single-Cell Transcriptomic Analysis Reveals the Developmental Trajectory and Transcriptional Regulatory Networks of Pigment Glands in *Gossypium bickii*." *Molecular Plant* 16, no. 4: 694–708. <https://doi.org/10.1016/j.molp.2023.02.005>.
- Tang, L., G. Li, H. Wang, et al. 2024. "Exogenous Abscisic Acid Represses Rice Flowering via SAPK8-ABF1-Ehd1/Ehd2 Pathway." *Journal of Advanced Research* 59, no. 35: 47.
- Thoma, S., Y. Kaneko, and C. Somerville. 1993. "A Non-Specific Lipid Transfer Protein From Arabidopsis Is a Cell Wall Protein." *Plant Journal* 3, no. 3: 427–436.
- Wang, D., X. Hu, H. Ye, et al. 2023. "Cell-Specific Clock-Controlled Gene Expression Program Regulates Rhythmic Fiber Cell Growth in Cotton." *Genome Biology* 24, no. 1: 49. <https://doi.org/10.1186/s13059-023-02886-0>.

- Wang, H., Y. Sun, J. Chang, et al. 2016. "Regulatory Function of Arabidopsis Lipid Transfer Protein 1 (LTP1) in Ethylene Response and Signaling." *Plant Molecular Biology* 91, no. 4: 471–484. <https://doi.org/10.1007/s11103-016-0482-7>.
- Wang, Y., Q. Huan, K. Li, and W. Qian. 2021. "Single-Cell Transcriptome Atlas of the Leaf and Root of Rice Seedlings." *Journal of Genetics and Genomics* 48, no. 10: 881–898.
- Wendrich, J. R., B. Yang, N. Vandamme, et al. 2020. "Vascular Transcription Factors Guide Plant Epidermal Responses to Limiting Phosphate Conditions." *Science* 370, no. 6518: eaay4970. <https://doi.org/10.1126/science.aay4970>.
- Wu, T., E. Hu, S. Xu, et al. 2021. "Clusterprofiler 4.0: A Universal Enrichment Tool for Interpreting Omics Data." *Innovation* 2: 100141.
- Xu, X., A. M. van Lammeren, E. Vermeer, and D. Vreugdenhil. 1998. "The Role of Gibberellin, Abscisic Acid, and Sucrose in the Regulation of Potato Tuber Formation In Vitro." *Plant Physiology* 117, no. 2: 575–584. <https://doi.org/10.1104/pp.117.2.575>.
- Yadav, R. K., T. Girke, S. Pasala, M. Xie, and G. V. Reddy. 2009. "Gene Expression Map of the Arabidopsis Shoot Apical Meristem Stem Cell Niche." *Proceedings of the National Academy of Sciences* 106, no. 12: 4941–4946. <https://doi.org/10.1073/pnas.0900843106>.
- Yang, B., M. Minne, F. Brunoni, et al. 2021. "Non-Cell Autonomous and Spatiotemporal Signalling From a Tissue Organizer Orchestrates Root Vascular Development." *Nature Plants* 7, no. 11: 1485–1494. <https://doi.org/10.1038/s41477-021-01017-6>.
- Yang, Z., E. K. Wafula, L. A. Honasas, et al. 2015. "Comparative Transcriptome Analyses Reveal Core Parasitism Genes and Suggest Gene Duplication and Repurposing as Sources of Structural Novelty." *Molecular Biology and Evolution* 32, no. 3: 767–790. <https://doi.org/10.1093/molbev/msu343>.
- Zeng, J., X. Li, Q. Ge, et al. 2021. "Endogenous Stress-Related Signal Directs Shoot Stem Cell Fate in *Arabidopsis thaliana*." *Nature Plants* 7, no. 9: 1276–1287. <https://doi.org/10.1038/s41477-021-00985-z>.
- Zhang, L., C. He, Y. Lai, et al. 2023. "Asymmetric Gene Expression and Cell-Type-Specific Regulatory Networks in the Root of Bread Wheat Revealed by Single-Cell Multiomics Analysis." *Genome Biology* 24, no. 1: 65. <https://doi.org/10.1186/s13059-023-02908-x>.
- Zhang, T. Q., Y. Chen, Y. Liu, W. H. Lin, and J. W. Wang. 2021. "Single-Cell Transcriptome Atlas and Chromatin Accessibility Landscape Reveal Differentiation Trajectories in the Rice Root." *Nature Communications* 12, no. 1: 2053. <https://doi.org/10.1038/s41467-021-22352-4>.
- Zhang, T. Q., Y. Chen, and J. W. Wang. 2021. "A Single-Cell Analysis of the Arabidopsis Vegetative Shoot Apex." *Developmental Cell* 56, no. 7: 1056–1074.e1058. <https://doi.org/10.1016/j.devcel.2021.02.021>.
- Zhang, T. Q., Z. G. Xu, G. D. Shang, and J. W. Wang. 2019. "A Single-Cell RNA Sequencing Profiles the Developmental Landscape of Arabidopsis Root." *Molecular Plant* 12, no. 5: 648–660. <https://doi.org/10.1016/j.molp.2019.04.004>.

Supporting Information

Additional supporting information can be found online in the Supporting Information section.